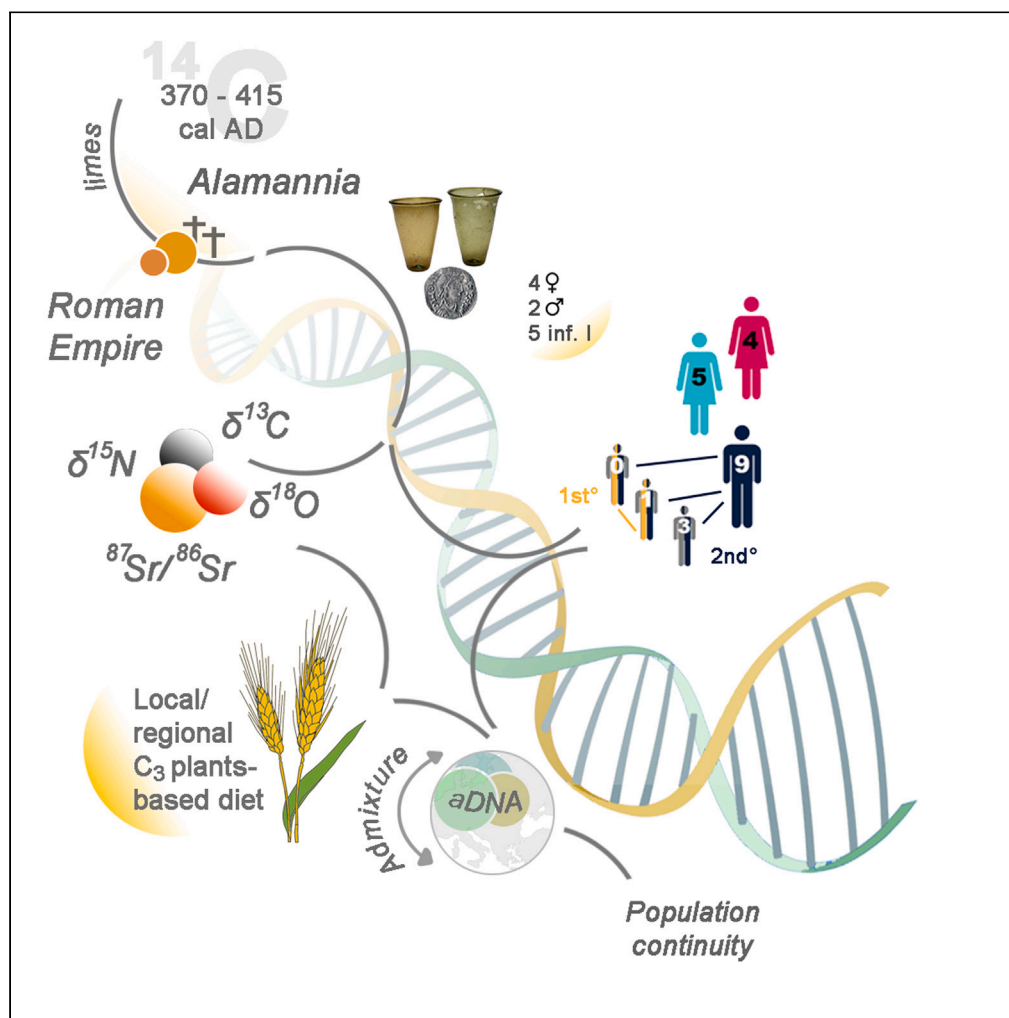


Article

Bioarchaeological analyses reveal long-lasting continuity at the periphery of the Late Antique Roman Empire



Margaux L.C. Depaermentier, Ben Krause-Kyora, Irka Hajdas, ..., Norbert Spichtig, Peter-Andrew Schwarz, Claudia Gerling

m.depaermentier@unibas.ch

Highlights

First Late Antique human isotope and aDNA data from the southern Upper Rhine Valley

Multidisciplinary approach revises the hitherto narrative at Basel-Waisenhaus

Bioarchaeology challenges the concept of population replacement in the Alamannia

This pilot study highlights important gaps in the current state of research

Depaermentier et al., iScience
26, 107034
July 21, 2023 © 2023 The Author(s).
<https://doi.org/10.1016/j.isci.2023.107034>

Article

Bioarchaeological analyses reveal long-lasting continuity at the periphery of the Late Antique Roman Empire

Margaux L.C. Depaermentier,^{1,8,*} Ben Krause-Kyora,² Irka Hajdas,³ Michael Kempf,⁴ Thomas Kuhn,⁵ Norbert Spichtig,⁶ Peter-Andrew Schwarz,¹ and Claudia Gerling^{1,7}

SUMMARY

The Basel-Waisenhaus burial community (Switzerland) has been traditionally interpreted as immigrated Alamans because of the location and dating of the burial ground – despite the typical late Roman funeral practices. To evaluate this hypothesis, multi-isotope and aDNA analyses were conducted on the eleven individuals buried there. The results show that the burial ground was occupied around AD 400 by people belonging largely to one family, whereas isotope and genetic records most probably point toward a regionally organized and indigenous, instead of an immigrated, community. This strengthens the recently advanced assumption that the withdrawal of the Upper Germanic-Rhaetian *limes* after the “Crisis of the Third Century AD” was not necessarily related to a replacement of the local population by immigrated Alamannic peoples, suggesting a long-lasting continuity of occupation at the Roman periphery at the Upper and High Rhine region.

INTRODUCTION

During the third to the fifth centuries AD, the European continent was characterized by rapid social, political, economic, and religious changes, both within and without the Roman Empire.^{1–3} Either interpreted as cause or consequence of those changes, the so-called barbarian invasions or migrations are usually seen as one of the key processes of the Late Antique and Early Medieval period, often referred to as the Migration Period.^{1,4–6} In this context, the comparison of “Romans” and “Germans” has traditionally played a major role in archaeological and historical research.^{7–10}

During this period, the area of present-day Basel (CH) was a socio-cultural melting pot because of its location at the river Rhine (Figure 1), which became the border (*limes*) of the Roman Empire after the abandonment of the Upper Germanic-Rhaetian *limes* around AD 260.^{11,12} A Roman military presence is still attested along the Rhine-*limes* through Valentinian’s fortification campaign around AD 374.^{13,14} In this context, the area was, at an administrative level, divided into a “Roman” part on the southern bank and a “German” or “Alamannic” part on the northern bank of the river Rhine from approximately AD 260 to AD 475.^{14–16} Both parts have been long considered culturally isolated within scholarly research.^{17,18}

This was also derived from the different Roman historical background on each riverside. During the first step of Caesar’s conquest of Gaul in the first century BC, the Roman occupation was extended up to the river Rhine in Northern Switzerland, whereas a military presence on the northern riverbank was not attested before AD 75.¹⁶ Around AD 160, the eastern limit of the Western Roman Empire was extended up to the Upper Germanic-Rhaetian *limes* and along the Danube river.¹⁹ However, this only lasted until the so-called “Crisis of the Third Century”, which led, in the years around AD 260, to the loss of the *Agri decumates* on the western side of the Rhine,^{11,13} including the part of present-day Basel referred to as Kleinbasel, where the study site presented here, Basel-Waisenhaus, is located.

Moreover, the traditional narratives of the Migration period derived from written sources still hold sway over the interpretation of the archaeological records at Basel, where the burial grounds (including the Basel-Waisenhaus site presented in this study and described in the Data S2) were associated with specific ethnic groups.^{20–23} However there has been recent work within Early Medieval archaeological research to revise the hitherto predominant comparison of ethnicity and material culture.^{1,7–10}

¹Department of Ancient Civilizations, Prehistoric and Early Historic and Provincial Roman Archaeology, Vindonissa Professorship, University of Basel, Petersgraben 51, 4051 Basel, Switzerland

²Institute of Clinical Molecular Biology, Kiel University, Rosalind-Franklin-Straße 12, 24105 Kiel, Germany

³Laboratory of Ion Beam Physics, ETH Zurich, Otto-Stern-Weg 5 HPK H31, 8093 Zurich, Switzerland

⁴Department of Geography, Physical Geography, Landscape Ecology and Geoinformation, Kiel University, Ludewig-Meyn-Str. 8, 24098 Kiel, Germany

⁵Aquatic and Isotope Biogeochemistry, Department of Environmental Sciences, University of Basel, Bernoullistrasse 30, 4056 Basel, Switzerland

⁶Archäologische Bodenforschung Basel-Stadt, Petersgraben 11, 4001 Basel, Switzerland

⁷Integrative Prehistory and Archaeological Science, Department of Environmental Sciences, University of Basel, Spalenring 145, 4055 Basel, Switzerland

⁸Lead contact

*Correspondence: m.depaermentier@unibas.ch
<https://doi.org/10.1016/j.isci.2023.107034>



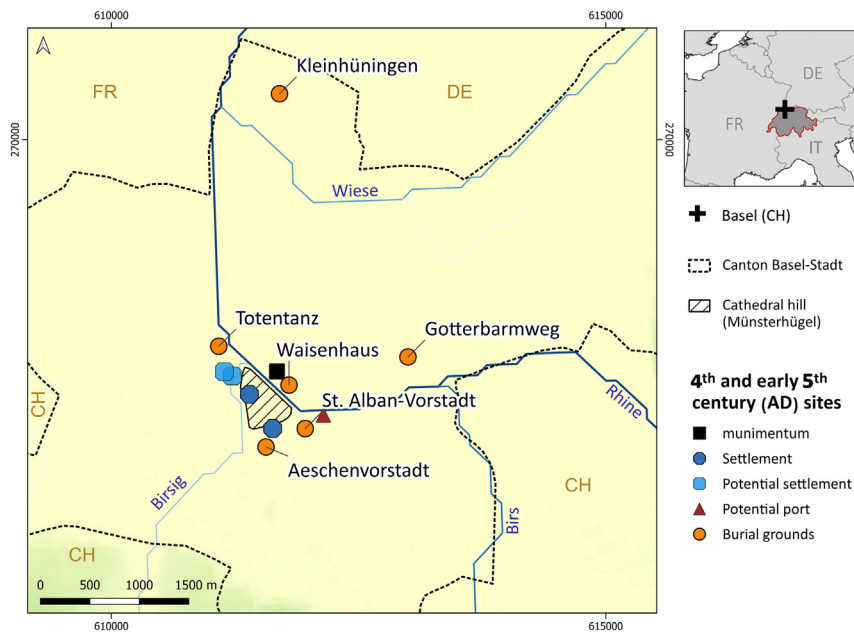


Figure 1. Location of the fourth and early fifth century AD sites, including settlements and burial grounds within the Canton of Basel-Stadt (CH)

CH = Switzerland, FR = France, DE = Germany.

To question these ethnically derived comparisons, there has been an increase in the use of bio-archaeological methods in Early Medieval archaeological research.²⁴ Genetic analyses (ancient DNA, hereafter referred to as aDNA) are often used to understand Early Medieval migration patterns,^{25–29} social structures,^{25,30–33} and the impact of Early Medieval migrations on the genetic composition of modern populations.^{34–36} In addition, strontium (Sr) and oxygen (O) isotope analyses have become common tools to trace potential mobility or migration events^{25,37–41} and the consequences of these migrations on the local population.^{40,42–47} Because the Migration Period is typically associated with the idea of foreign people with differing cultural and dietary practices deliberately and/or violently intruding on a local society,^{25,44,47,48} carbon (C) and nitrogen (N) isotope analyses may help to trace changes in dietary habits caused by migration and acculturation processes.^{40,43,47,49}

In this article, we carried out aDNA, as well as, C, N, O, and Sr isotope analyses on 11 individuals from the Basel Waisenhaus burial ground (Figure 2) to challenge traditional narratives of several migration waves from the East. Because most individuals were buried without grave goods, additional radiocarbon dating was performed to examine the validity of the interpolated archaeological dating of the Basel-Waisenhaus burial place to the first half of the fifth century AD. Based on the fact that the isotope composition of human (and animal) skeletal tissues is derived from the individual's diet and hence from the environmental settings from which the food^{50–53} and drinking water^{54–56} originate, a reconstructed model of potential land-use was carried out based on environmental explanatory covariates. This combination of methods fosters the understanding of local to supra-regional mobility patterns and socio-economic organization in a highly dynamic period of socio-cultural development.

RESULTS

The results of the radiocarbon dating, the aDNA analyses as well as the C, N, O, and Sr isotope analyses are listed in the Table S1. The calculated mean values and standard deviations are summarized in Table 1.

Land-use model

The environmental settings used as basis for the model are described in the Data S3. The geological and isotopic (Sr) settings are depicted in Figure 3. From the environmental and land-use model, the potential land-use zones are located in close vicinity to the reconstructed settlement and spread toward the north along the river Wiese (Figure 4). Considering alluvial soils on the lower terraces of the channel floodplains, these fertile

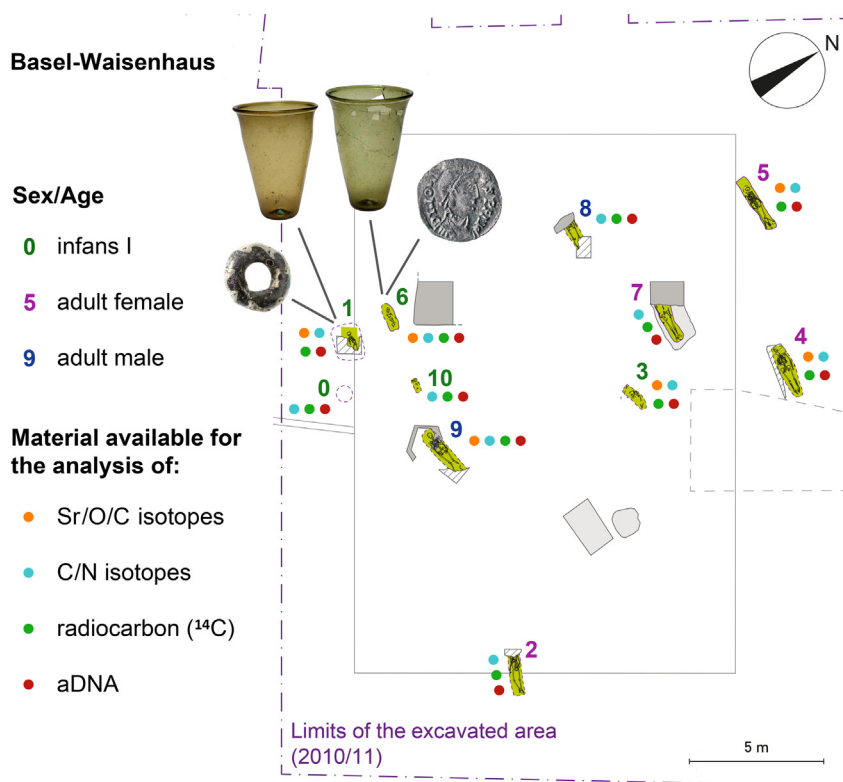


Figure 2. Plan of the burial ground with information about sex, age, grave goods, and the material available for the isotope and aDNA-analyses

Modified by M. Depaermentier after Baumann et al.,²⁰ Figure 7. Images of grave goods by Archäologische Bodenforschung Basel-Stadt. (See also [Data S2](#) for a description of the burial ground).

soils would promote intensive agricultural exploitation and simultaneously allow for irrigation measures during subsequent drought periods. Most of the highly suitable sites are located within a 1 km distance of the settlement, which aligns with the theory underlying the activity spheres of subsistence farming of this article.⁵⁹ Following the expectations of the given hypothesis, the land-use suitability decreases toward the other side of the river Wiese. Crop production on both sides of the river cannot be ruled out. There is an increased risk of harvest loss on the northern side of the river after heavy rain events, drought periods, or damage caused by game. Finally, the model, which considered environmental variability at the microlocal level, enables a validation of the Sr isotope baseline suggested by D. Brönnimann and colleagues for Basel-Gasfabrik.⁵⁷

Radiocarbon dating

The results of radiocarbon dating performed on the eleven bones that were analyzed in this study are presented with a 95.4% probability ([Table S1](#)) and were calibrated in the OxCal software v4.4.4⁶⁰ using the last published calibration curve IntCal20: Northern Hemisphere.⁶¹ The calibrated dates show individual ranges from minimum AD 241 (grave 1) and maximum AD 403 (grave 9) to minimum AD 404 (grave 4) and maximum AD 538 (grave 9), corresponding to a total range of approximately 300 years ([Table S1](#)). However, the kernel density estimation (KDE) model ([Figure 5](#)) reveals high-frequency noise from these wide ranges that are because of a wiggle in the calibration curve for the oldest part and to a plateau in this curve for the most recent part of this range.⁶² After the algorithm removed this noise, the single-modelled dates showed a minimum at AD 337 (grave 1) and a maximum at AD 434 (grave 9), with a most probable total range of 40 years spanning from AD 370 to AD 410 (95.4%, Agreement Indices of the model: 96.4).

The separation of bones of children and adults shows slightly different distribution with a maximum for children centered at AD 400, and the maximum for adults shifted toward the older ages by some 20–30 years. This is in agreement with the slow turnaround time (20–30 years) of bones^{63–65} and the fact that teeth register the ¹⁴C signal from the early years. Thus, all the graves might be from the time period centered at AD 400.

Table 1. Summary statistics for isotope data

Basel-Waisenhaus	$^{87}\text{Sr}/^{86}\text{Sr}$	$\delta^{18}\text{O}_\text{C}$ (‰ VPDB)	$\delta^{13}\text{C}$ (‰ VPDB)	$\delta^{15}\text{N}$ (‰ AIR)
sample (incl. G0)				
n ind. (samples)	6 (9)	6 (9)	11 (11)	11 (11)
mean	0.7093	−4.9	−18.6	9.6
1 σ	0.0006	0.5	0.7	1.3
min	0.7088	−5.6	−19.3	8.3
max	0.7102	−4.2	−16.8	12.1
sample (excl. G0)				
n ind. (samples)	6 (9)	6 (9)	10 (10)	10 (10)
mean	0.7093	−4.9	−18.8	9.4
1 σ	0.0006	0.5	0.4	1.1
min	0.7088	−5.6	−19.3	8.3
max	0.7102	−4.2	−18.2	11.4
adults				
n ind. (samples)	3 (6)	3 (6)	6 (6)	6 (6)
mean	0.7095	−5.1	−18.8	9.0
1 σ	0.0007	0.4	0.5	0.6
min	0.7088	−5.6	−19.3	8.4
max	0.7102	−4.6	−18.2	10.1
infants (incl. G0)				
n ind. (samples)	3 (3)	3 (3)	5 (5)	5 (5)
mean	0.7090	−4.7	−18.3	10.4
1 σ	0.0002	0.5	1.0	1.6
min	0.7089	−5.2	−19.2	8.3
max	0.7091	−4.2	−16.8	12.1
infants (excl. G0)				
n ind. (samples)	3 (3)	3 (3)	4 (4)	4 (4)
mean	0.7090	−4.7	−18.7	10.0
1 σ	0.0002	0.5	0.5	1.4
min	0.7089	−5.2	−19.2	8.3
max	0.7091	−4.2	−18.2	11.4

Mean, 1 σ , minimum, and maximum values of the $^{87}\text{Sr}/^{86}\text{Sr}$, $\delta^{18}\text{O}_\text{C}$, $\delta^{13}\text{C}$, and $\delta^{15}\text{N}$ values for the whole sample, the adults, and the infants from Basel-Waisenhaus (see [Table S1](#) for detailed raw data).

aDNA analyses

Overall, the preservation of the aDNA in the various samples was generally very good, with the exception of the samples from graves 6, 7, and 8, which were poorly preserved ([Table S1](#)). There was no aDNA preservation given in the sample collected from the burial 10. In total, the results of the other seven individuals can be considered reliable. There was no sign of contamination in any of the samples, and the typical damage pattern used as an authentication criterion for aDNA was present (see columns “dmg 5p first pos” and “dmg 3p third pos” in [Table S1](#) and [Figure S1](#)).

The successful determination of the genetic sex of seven of the eleven individuals suggests that this burial group consisted of a minimum of three males (burials 0, 3, 9) and four females (burials 1, 2, 4, 5). These results only match the results of the anthropological analysis for individuals 2, 3, 6, and 9, while they gave contradictory results for individuals 1 and 4. Also, additional information was garnered for the unsexed individuals 0 and 5. Because of the bad preservation of aDNA in the samples from graves 7, 8, and 10, no genetic sex could be determined.

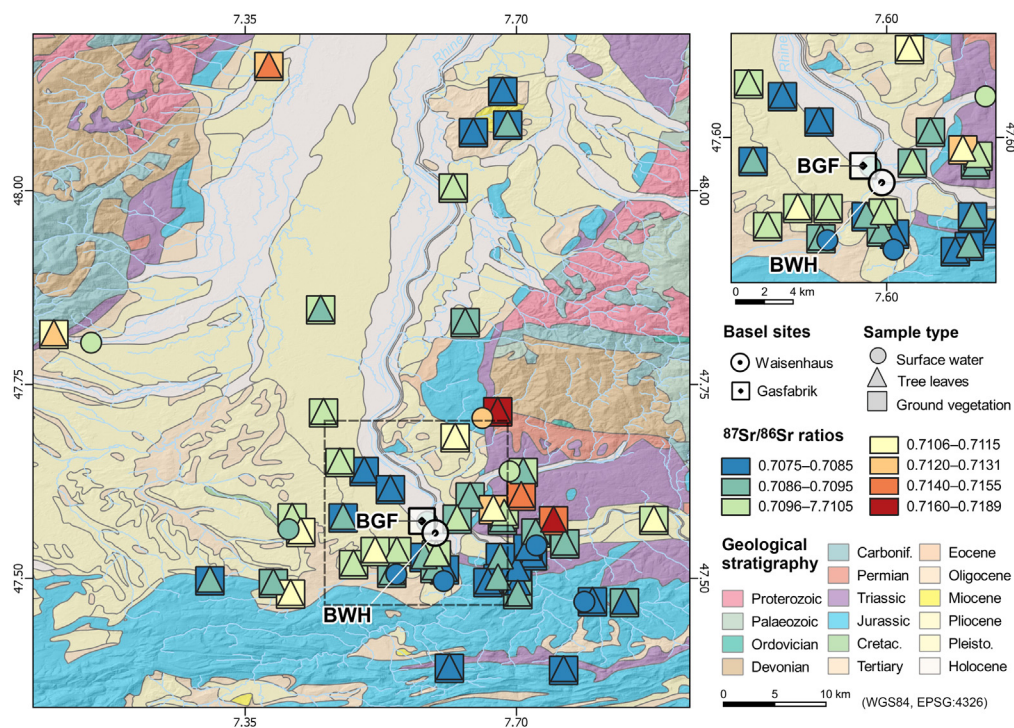


Figure 3. Strontium isotope baseline data and geological background

Geological map of the Upper Rhine Valley with the location of Basel-Gasfabrik (BGF) and Basel-Waisenhaus (BWH) and the baseline samples collected and analyzed by D. Brönnimann and C. Knipper^{57,58} for the determination of bioavailable Sr composition in the region (left).

The black rectangle shows the map section to the right. An interpolated Sr isoscape of the region is available in Brönnimann et al. (2018, Figure 3).⁵⁷ Sr isotope data are available from the supplementary tables by D. Brönnimann and C. Knipper.^{57,58} The digital elevation model (DEM) is available from swisstopo. The geological map is downloaded from the INSPIRE under Creative Commons Attribution 4.0 International (CC BY 4.0) license. (See also Data S2 for a description of the environmental settings).

The determination of the mt- and y-haplotypes revealed the presence of four different mt-haplotypes: U2e2a1a (graves 0, 1, 6), H11a (graves 9, 3), H1c5 (grave 5), and I2 (grave 4). At least two different y-haplotypes could also be attested: I2a2a2a (grave 3) and I2c2 (grave 0 and 9). The complementary results of the analysis of the genome-wide variants showed second-degree for the individual from grave 9 to the individuals from graves 0, 1, and 3. This means that there is one other family member between grave 9 and graves 0, 1, 3, respectively, i.e., grave 9 shares 25% of the genomes of each of these persons. This represents a relationship such as a grandparent and grandchild, half-siblings, double-cousins, or aunt/uncle and niece/nephew. Furthermore, a first-degree relationship exists between graves 0 and 1 (Table S2).

The results of the PCA plot (Figures 6 and S2), f3 statistics (Figure S3), and admixture plots (Data S1) suggest that the burial community in Basel-Waisenhaus corresponds to a particularly homogeneous group descending from only one population. The individuals from grave 2 and 5 represent the only recurrent outliers. The current resolution suggests that the Basel-Waisenhaus individuals are not connected with modern and past populations from Southern Europe but instead have more connections to Western, Central, and Northern Europe with respect to both the ancient and modern references. The admixture plots (Data S1) and the f3 statistics (Figure S3) also support the analogy with the latter group.

Strontium and oxygen isotopes

The $^{87}\text{Sr}/^{86}\text{Sr}$ ratios of the human dental enamel sampled from the Basel-Waisenhaus individuals (11 samples from 6 individuals) range from 0.7088 to 0.7102 (Table S1) with a mean value of 0.7093 ± 0.0006 (1 SD) (Table 1). The two bones exhibited a ratio of 0.7090 and 0.7091 respectively, which is very similar to the isotope composition of the sampled deciduous teeth as well as the first and third molar of the female

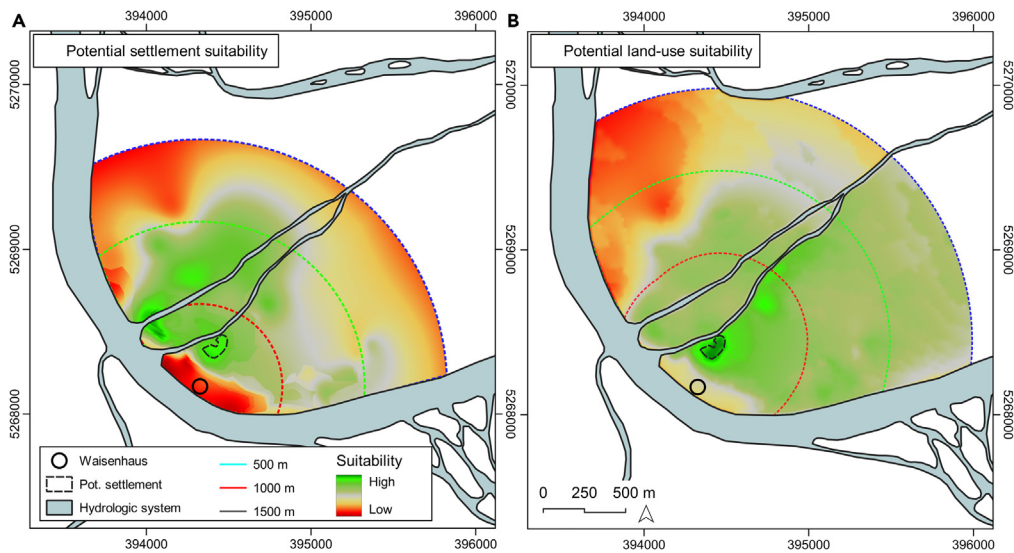


Figure 4. Predictive land-use and settlement model

Predictive model for potential settlement location (A) and agricultural exploitation (B) in the predicted complementary region of the graveyard Basel-Waisenhaus. The model is based on soil suitability, potential waterlogging and groundwater level, geological units, as well as landscape permeability, including the reconstructed pre-modern channels of the river Wiese. (See also [Data S2](#) for a description of the environmental settings).

from grave 4 and to the third molar of the male from grave 9 (mean value: 0.7090 ± 0.0001 ; see [Table 1](#)). These samples perfectly match the so-called local I baseline range (0.7083–0.7093) estimated by D. Brönnimann, C. Knipper, and colleagues^{57,58} ([Figure 7](#)). This range reflects the Sr isotope value of arable land mainly exploited by the inhabitants of the Late La Tène settlement at Basel-Gasfabrik – and at Basel-Waisenhaus based on the land-use model. The first molar of the male from grave 9 and both teeth of the female in grave 5 show $^{87}\text{Sr}/^{86}\text{Sr}$ ratios on average 0.001 higher than the mean value of the other individuals. Nonetheless, these values still fit in the so-called local II Sr isotope baseline range (0.7093–0.7114).^{57,58} The range is thought to correspond with the arable land in the surroundings of Basel-Gasfabrik – including the surroundings of Basel-Waisenhaus. However, this wide range resulting from the heterogeneous environmental settings in the area ([Figure 3](#)) is not just specific for Basel but can be found in surrounding regions^{66–71} and other areas across Europe.^{72–77}

The $\delta^{18}\text{O}$ values of the tooth enamel carbonate range from -5.6 to -4.2‰ with a mean value of $-5.0 \pm 0.5\text{‰}$ (1 SD). To compare these results with the O isotope baseline range in tooth enamel phosphate (15.7–17.2‰) estimated by C. Knipper for the Basel-Gasfabrik project,⁵⁸ we first converted the carbonate data into $\delta^{18}\text{O}_{\text{SMOW}}$ according to the [Equation 1](#) suggested by Coplen and colleagues.⁷⁸ Second, we converted those results into phosphate values according to the [Equation 2](#) suggested by Iacumin and colleagues.⁷⁹

$$\delta^{18}\text{O}_{\text{SMOW}} = 1.03091 \times \delta^{18}\text{O}_{\text{C}} + 30.91 \quad (\text{Equation 1})$$

$$\delta^{18}\text{O}_{\text{P}} = 0.98 \times \delta^{18}\text{O}_{\text{SMOW}} - 8.5 \quad (\text{Equation 2})$$

The converted $\delta^{18}\text{O}_{\text{P}}$ values range from 16.1 to 17.6‰ with a mean value of $16.7 \pm 0.4\text{‰}$ (1 SD) and match overall the local O isotope baseline range (15.7–17.2‰) estimated at Basel by C. Knipper and colleagues.⁵⁸ This local O isotope baseline range is based on modern precipitation data from Weil am Rhein and on local and regional surface water. It is noteworthy that the infants 1 and 6 are slightly above the upper limit of this range ([Figure 7](#)).

Carbon and nitrogen isotopes

All eleven human skeletons provided sufficient bone collagen for C and N stable isotope analyses. The detailed results of the C and N isotope analyses obtained from bone collagen are listed in [Table S1](#) and represented in [Figure 8](#). The C/N ratios ranged from 3.1 to 3.2, indicating good collagen preservation of

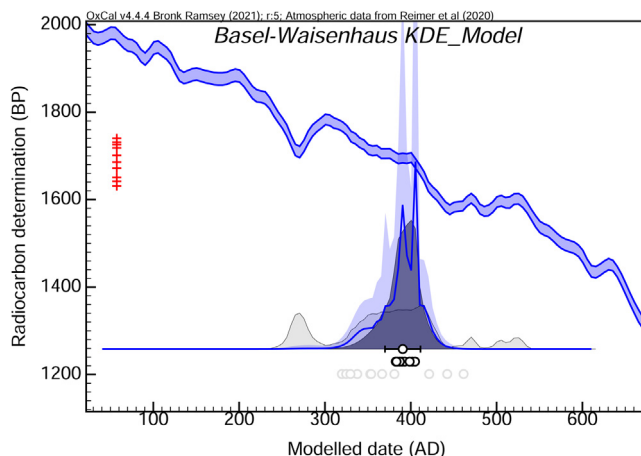


Figure 5. KDE model of the eleven radiocarbon dates from Basel-Waisenhaus, using OxCal v.4.4.4

The KDE shows a most probable range spanning from approximately AD 370 to AD 410 (95.4%, A_{model} : 96.4). The horizontal bars represent the mean \pm 1 SD. See also [Table S1](#) for detailed raw values.⁶⁰

these samples.^{82,83} However, the percentage of C in the bone collagen from grave 2 is low (26.9%). The $\delta^{13}\text{C}$ (‰ PDB) and $\delta^{15}\text{N}$ (‰ AIR) values of the whole sample range from -19.3 to -16.8 ‰ (mean value -18.6 ± 0.7 ‰, 1 SD) and from 8.3 to 12.1 ‰ (mean value 9.6 ± 1.3 ‰, 1 SD) (Table 2). The infant from grave 0 exhibits the highest $\delta^{13}\text{C}$ and $\delta^{15}\text{N}$ and is an obvious outlier in this sample (Figure 8). The lowest $\delta^{13}\text{C}$ and $\delta^{15}\text{N}$ values correspond to the female from grave 5 and to the infant from grave 3 respectively. The infants from graves 6 and 10 have $\delta^{15}\text{N}$ values up to 2.4 ‰ higher than the mean value of the adults (9.0 ± 0.6 ‰, 1 SD).

No Early Medieval baseline sample was available for this study. Hence, we considered the Late Iron Age faunal and plant samples collected at the Basel-Gasfabrik site⁸⁰ as well as the medieval faunal data from the Barfüsserkirche in Basel (11th century)⁸¹ as comparative data. The $\delta^{13}\text{C}$ and $\delta^{15}\text{N}$ values of adult individuals from the Basel-Waisenhaus site showed an offset of 2.5 and 2.2 ‰, respectively, compared to the Iron Age herbivores from the Basel-Gasfabrik site (Figure 8, Table S2), and an offset of 2.5 and 3.5 ‰ compared to the medieval domestic herbivores from the Basel-Barfüsserkirche (11th century).⁸¹

Additional $\delta^{13}\text{C}$ values were obtained from the same dental enamel sample analyzed for Sr and O isotope composition (Table S1). The $\delta^{13}\text{C}$ values measured in dental enamel varied from -10.7 (grave 3, tooth 84) to -13.8 ‰ (grave 5, tooth 36). The mean value is -12.0 ± 1.1 ‰ (1 SD). On average, the tooth $\delta^{13}\text{C}$ value is 6.7 ± 1.0 ‰ (1 SD) more positive than the bone collagen $\delta^{13}\text{C}$ values of the same individual, with a minimum offset of 5.0 ‰ for grave 4 and a maximum offset of 8.0 ‰ for grave 1.

DISCUSSION

A homogeneous community

Radiocarbon dating allowed for a precise chronology of this burial place. Instead of being restricted to the second quarter of the fifth century as assumed from the interpolated dating of the grave goods in burial 1 and 6,²⁰ the calibrated and modeled radiocarbon dates highlight that the use of this burial place may have already started during the second half of the fourth century AD and lasted approximately 40 years – if the KDE model is taken into account (Figure 5). Although the focus is clearly around AD 400 when considering the age difference between adult and infant individuals, the upper limit of the modeled range (AD 410) should be slightly extended to integrate the siliqua imitation found in grave 6, which gives a *terminus post quem* around AD 411–413 at least for this burial. Moreover, the determination of the mt- and y-haplotypes, as well as the analysis of the genome-wide variants (Tables S1 and S2), stress that even though the limits of the burial ground were probably not reached during the excavation, at least four individuals (graves 0, 1, 3, and 9) share a second-degree kinship relationship.

The infant in grave 6 has a similar basis for its mt-haplotype (U2e2a1a) to the infants in grave 0 and 1, who are buried nearby. It also has similar grave goods compared to infant 1. Its aDNA was not well preserved

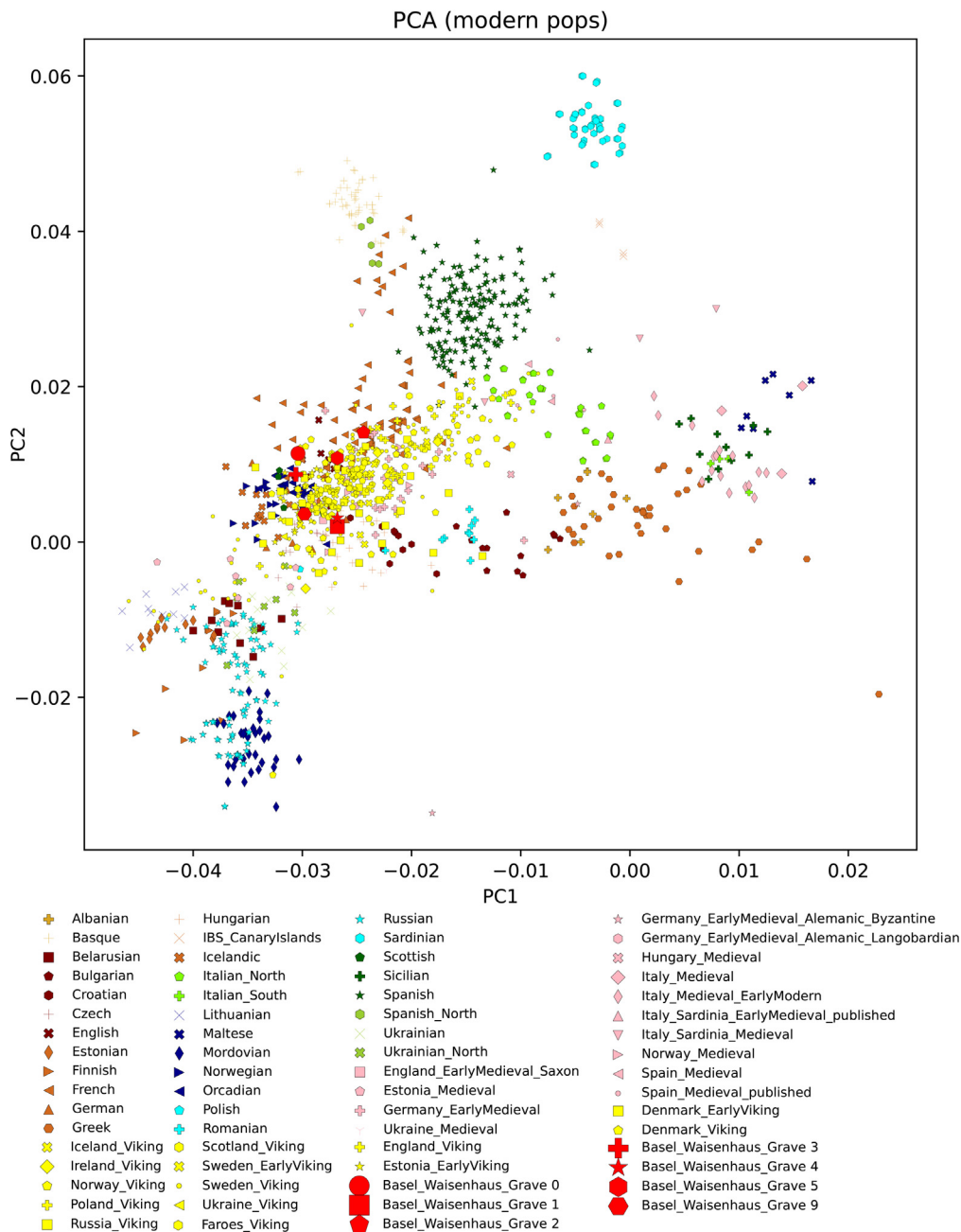


Figure 6. PCA plot

The PCA shows the burial community of Basel-Waisenhaus clustering together with modern central and northern Europeans (e.g. English, French, Germans), as well as Early Medieval populations that occupied these regions (see also [Figure S2](#) for a larger comparison sample and [Table S1](#) for detailed raw data).

enough to trace any kinship relationship, but a close link may be assumed. There are no data for infant 10 and adults 7 and 8. The only real outliers are females 2 and 5, who show different mt-haplotypes. These females might belong to another family or come from another community, even though the concept of *familia* also includes individuals beyond the relatives through blood. In this case, the marginal position of both outlier burials within the burial place is noteworthy and might suggest that they had a specific status in life or death. The presence of at least one family and the short period of deposition strengthen the idea that this burial ground was used by a homogeneous community, as also expected from the overall uniformity of

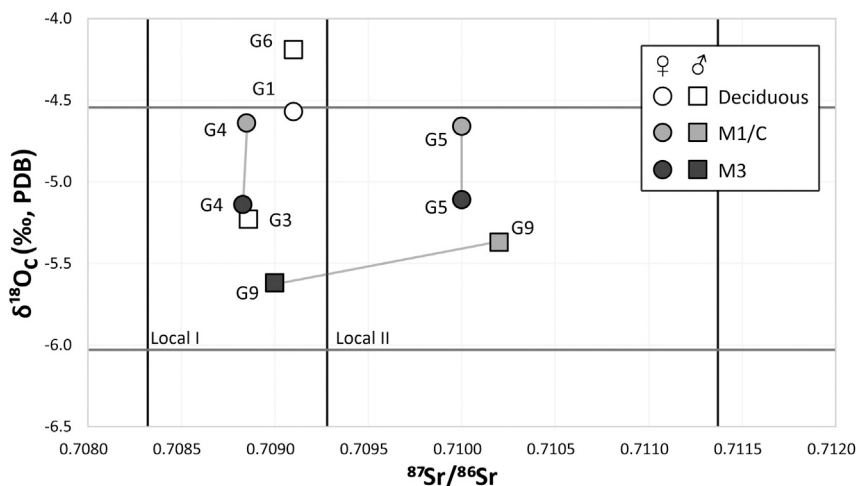


Figure 7. Strontium and oxygen isotope data

Results of the strontium and oxygen isotope analyses compared to the strontium and oxygen isotopes local ranges determined by C. Knipper, D. Brönnimann and colleagues for the Basel-Gasfabrik project^{57,58} (see also Table S1 for detailed raw data).

the burial practices.²⁰ The PCA plots also emphasise this aspect, in which only the female 2 can be considered a slight outlier.

The $^{87}\text{Sr}/^{86}\text{Sr}$ values of the Basel-Waisenhaus individuals mainly fit within the local I range determined by C. Knipper and D. Brönnimann for the Basel-Gasfabrik site.^{57,58} The female 5 and male 9 exhibit slightly different $^{87}\text{Sr}/^{86}\text{Sr}$ ratios in their early mineralized teeth, which nevertheless still match the Basel-Gasfabrik's local II range (Figures 3, 4, and 7). If we consider the closest place with similar Sr isotope composition as the most probable place of origin, this means that either both individuals were born in Basel's direct surrounding region or that their food came from another parcel of land in or around Basel compared to the other members of the group.

Moreover, the $\delta^{18}\text{O}$ values show that except for the infant 6 (G6), all individuals fit into the local O isotope range determined by C. Knipper for the Basel-Gasfabrik site⁵⁸ (Figure 7). The infant 6's deciduous tooth exhibits an offset of 0.4‰ compared to the upper limit of the local range and 0.7‰ compared to the mean value of the adults, respectively (see Table 1). However, the $\delta^{18}\text{O}$ ratios measured in deciduous teeth and the first permanent molars might be biased by the breast-feeding effect if the individual consumed breast milk (which is enriched in ^{18}O) during the first months or years of its life.⁸⁴ This may lead to an offset of up to 1.3‰,⁸⁴ whereas a more significant or inverted offset between the first permanent molar or deciduous teeth and the later mineralized tooth could be considered as an indication of mobility.⁸⁰ The O isotope composition of this individual's tooth might instead indicate the potential influence of breastfeeding than evidence for mobility. It is supported by the $\delta^{15}\text{N}$ values from its femur collagen, which shows the expected offset related to the trophic level of mother milk consumption. Overall, the results of the Sr and O isotope analyses point toward a local organization of this burial community.

Regarding the dietary habits of those examined, the $\delta^{13}\text{C}$ and $\delta^{15}\text{N}$ values measured in the femur collagen of each individual reveal an overall omnivorous diet (Figure 8). The absence of a contemporaneous baseline and the differences in climatic conditions,⁸⁵ as well as potential differences regarding agricultural practices between the Iron Age, the Late Antiquity, and the Middle Ages, does not allow for the use of baseline values from Basel-Gasfabrik and Basel-Barfüsserkirche for a more precise investigation on dietary habits. A $\delta^{13}\text{C}$ value of -18.0‰ is generally acknowledged as a theoretical threshold distinguishing a C_3 - from a C_4 -plants-based diet in human bone collagen.^{44,47,80,86} Because most individuals exhibit more negative $\delta^{13}\text{C}$ values, we can assume that the diet was mainly based on C_3 -plants at Basel-Waisenhaus, without evident disparities among the group.

The infant 0 represents the only outlier with considerably higher $\delta^{15}\text{N}$ and $\delta^{13}\text{C}$ values compared to the other individuals. Both the consumption of marine fish or a protein-rich diet based on C_4 -plants are no

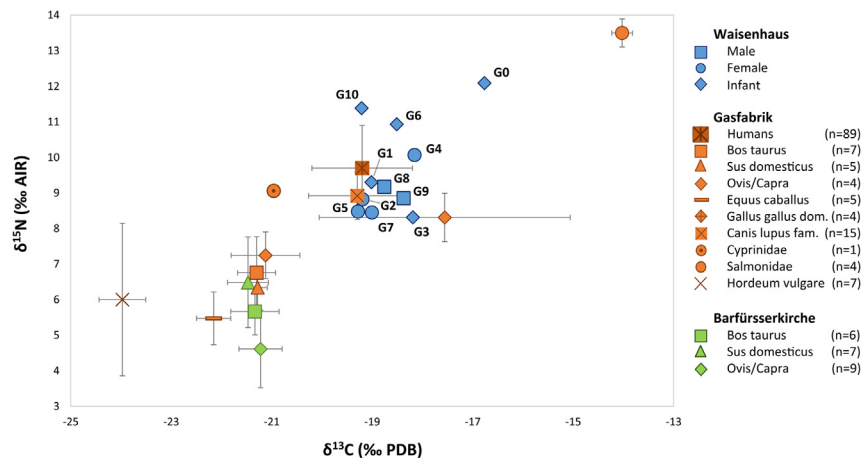


Figure 8. Carbon and nitrogen isotope data

$\delta^{13}\text{C}$ and $\delta^{15}\text{N}$ values of the adult males, adult females, and infants from Basel-Waisenhaus (see Table S1 for detailed raw data) compared to the mean $\delta^{13}\text{C}$ and $\delta^{15}\text{N}$ values isotope values (± 1 SD) from the Late Iron Age site at Basel-Gasfabrik⁸⁰ and from the Medieval (11th century AD) site at Basel-Barfüsserkirche⁸¹ (see Table 1 for mean and SD values).

reasonable explanations in Basel-Waisenhaus for this child. Also, even though this may not hold true for his mother not present in the cemetery, because he was breastfed, it might be surprising to see no residue from this diet in its sibling's bone (grave 1). Because the child died between the 6th and the 12th month after birth, the extreme values might have been caused by a severe disease or stress situation. Even though the impact of malnutrition, diseases, and other stress factors on the isotope composition of human tissues is still difficult to assess,^{87–89} it is possible that the extreme C and N isotope ratios measured in the bone collagen of infant 0 were related to a health issue^{90–96} or potentially a special diet meant as medicine.

Immigrated Alamans or indigenous Romans?

The revision regarding the chronology of this burial place points out that this community may be related to the so-called *munimentum* located about 150 m to the West of Basel-Waisenhaus. This Late Antique fortress was built in AD 374 during the fortification campaign of the Rhine *limes* led by the Roman emperor Valentinian I.¹³ After having “devastated some districts of the Alamanni” (*vastatos aliquos Alamanniae pagos*), he stayed on July 10th at a fortified camp (*munimentum*) called *Robur prope Basiliam*,⁹⁷ i.e., in Kleinbasel. Even though the toponym *Robur* probably first designated an imperial settlement (*statio, mutatio* or *mansio*), this place still played an important role in Late Antiquity.^{98,99} In this context, Ammianus explicitly referred to the civilian population living in the vicinity of the *munimentum* as *accolae*, i.e. as neighbors or *residents* – and not as inhabitants (*incolae*). The community buried in the Waisenhaus area could therefore have been part of the Roman provincial population that remained after the fall of the *limes* in the area on the northern riverbank.¹³

It is, furthermore, assumed that part of the soldiers from the Roman army based in the *castrum* on the opposed riverbank were positioned in the *munimentum*.^{13,14,100} The severity of (often healed) injuries and particularly the three fatal blows caused by a sharp weapon, such as an axe or a sword, on the skull of the robust male in grave 9 (Figure 9)²⁰ may support the interpretation of this burial place as belonging to a military place, such as the *munimentum*. Similar cuts are relatively frequent in other burial places related to Late Roman *castra* in the region.^{101–103} This is in contrast to the low proportion of males ($n = 2$) compared to females ($n = 4$) and children ($n = 5$) and the absence of military features such as weapons or *militaria* within the graves being less common. Though this might be related to the small number of individuals, to the probably yet unknown limits of the burial area, and to the perturbation of the graves from the modern period onwards.²⁰

Thus, the nature of the connection between Basel-Waisenhaus and the *munimentum* is difficult to assess. Moreover, both written sources and archaeological records indicate that not only Romans but also Germans – including “Alamans” – were involved in the Roman army, especially during the fourth and fifth centuries AD.^{4,6,104–106} Hence, even if the Basel-Waisenhaus individuals were affiliated with the military



Figure 9. Three blows on the skull of the robust male buried in grave 9 were caused by a sharp weapon that instantly led to the death of this individual

© Photo: Philippe Saurbeck, Archäologische Bodenforschung Basel-Stadt, modified by Margaux Depaermentier.

munimentum, this would give no information about their belonging to “Roman” or “German/Alamannic” groups. Even though the presence of drinking glasses and a Charon’s obol as sole grave goods rather suggest a relation to the Roman tradition.^{107–109}

In general, this question can be considered inadequate and obsolete because the limits and the lack of pertinence of the traditional identification of cultural groups, ethnic categories, and identity through the study of the material culture has been generally disclosed in the last decades.^{1,7,8,10,110–113} Nevertheless, the results of the isotope and aDNA analyses provide new insights into the potential origin of the individuals buried in Basel-Waisenhaus. First, the isotope compositions of the dental enamel sampled at Basel-Waisenhaus match the local I and, to some extent, the local II range at Basel.⁵⁸ Thus, we can reject the hypothesis that this group was constituted of immigrated people.²⁰

This assumption is also supported by the $\delta^{13}\text{C}$ values from both the bone collagen and the dental enamel, which point toward a local C_3 -plant-based diet during all individuals’ childhood and last years of life. Even though millet is already attested sporadically in this region from Prehistory onwards, its consumption remains limited. In the surrounding regions, including both the Alsace and Southern Germany, the Late Antique and Early Medieval diet is based chiefly on C_3 -plants as well,^{41,49,67,114–116} whereas C_4 -plants inputs are usually either limited to small amounts¹¹⁷ or to a few (possibly foreign) individuals.^{49,118,119} In those cases, an origin from southern^{39,42,44,47} or eastern Europe was assumed,^{25,40,43,120} where the consumption of millet is more frequently attested.^{45,121} The diet at Basel-Waisenhaus, thus, corresponds to the regional expectations.

Moreover, the results of the ancient DNA analyses indicate that the community was most likely indigenous, in comparison to modern populations and the extant Early and Late Medieval populations, suggesting a close relationship to populations from western and northern Europe (see Figures 6, S2, and S3, Data S1). An exact assignment to a regional group, e.g. origin from the eastern or western bank of the Rhine, is not possible because of the lack of comparative data. Furthermore, it must be emphasized that the quality and resolution of the data are partly quite low and that the analyses did not yield any results for four individuals (i.e., 36%). A significant issue in this context is the particularly high mobility and, thus, admixture rate within central Europe from the Iron Age onwards, which limits the potential to assess the origin of Early Medieval populations.^{47,58,122,123} When considering the two drinking glasses found in graves 1 and 6, whose type is also documented in Northern/Central Gaul,^{20,124} at least a specific contact between this area and Basel can be assumed during the Late Antiquity. However, the presence of such objects in burials at Basel is no evidence of any form of migration from this northwestern region. When combined with the archaeological records, a genetic and cultural link with places within the northern part of the Western Roman

Empire is most likely. However, neither the isotope and aDNA analyses nor the archaeological context can provide any information about the ethnic background and identity of past communities.

It is particularly important to stress that neither the archaeological nor the isotope and genetic background of the individuals from Basel-Waisenhaus exclude the hypothesis that these could be descendants of earlier generations of immigrated people. This is an important point because it is traditionally assumed that people referred to as “Alamans” moved to this area in several waves between the end of the third and fifth centuries.^{11,12,15,125} However, recent research suggests that the term “Alamans” was not, in the first place, the name of a specific barbarian group but rather a new administrative designation for the people living in the no-longer-Roman *A. decumates*.^{6,15,16,126,127} It is, therefore, no longer considered as historically attested that one can expect newcomers on the northern riverbank from AD 260 onwards.

Long-lasting continuity

To start at the burial-ground-scale, the use of the Basel-Waisenhaus burial place over approximately two generations, the uniformity of the burial practices, and the kinship relationships shown by archaeological, genetic, and radiocarbon data first indicate a strong continuity within the burial place. Moreover, the genetic background of this burial community and the isotope composition of their skeletal remains indicate that the Basel-Waisenhaus individuals represented most probably a local population. Thus, this study provides the first possible evidence for the presence of indigenous people on the northern (i.e., “non-Roman”) riverbank at Basel, not only after the loss of the *A. decumates* around AD 260,^{11,13} but even after the fortification campaign led by the Western Roman Emperor Valentinian I in the second half of the fourth century AD.^{13,14}

In this context, the above-mentioned potential link between Basel-Waisenhaus and the *munimentum* could imply a possible relation to the Roman army. However, as already mentioned, this relationship would not inform about any (ethnic) affiliation to “Roman” or “German” groups. These burials probably mainly represent a civil community, including only one evidence of military injury – or interpersonal violence (grave 9). The results most probably support the hypothesis that this former Roman region and its inhabitants were not referred to as *Alamannia* and *Alamanni*, respectively, from AD 289 onwards because of the invasion or migration of “Alamannic people” after the shift of the *limes* to the river Rhine, but rather because of the change of this area’s administrative meaning from a Roman perspective.^{6,126,127}

Furthermore, the genetic composition of the Basel-Waisenhaus community was not only primarily similar to present-day communities from Western/Central Europe but also significantly different from the modern populations of Italy or Spain (Figures 6, S2, and S3, Data S1). This is particularly noteworthy when considering the Roman history of this research area described in the introduction. Consequently, even though the presence of the Roman army coming from Northern Italy is assumed on the northern riverbank at least for the period between the middle of the first and the middle of the third century AD,¹⁶ the genetic background of the Basel-Waisenhaus burial community reveals the probability that the Roman conquest did not lead to any population change. Certainly, a larger sample would be required to test this hypothesis.

Limitations of the study

Two limitations of this study must be considered. Even if the analyzed individuals represent the total number of the burial community at Basel-Waisenhaus, the sample size remains small and cannot be considered fully representative of the Late Antique society at Basel. The aDNA analysis, however, adds an important new dimension to the understanding of local social interactions. Furthermore, this sample lacks comparative data from the assumed “Roman” side of the *limes*, whereas the potential link to the *munimentum* may represent a biased context on this presumably “Germanic” riverside. A diachronic approach including a larger sample size ($n = 150$) and individuals from both sides of the river Rhine is currently underway (SNSF, project nr. 100011 208060).

The second issue concerns the equifinality of isotope data and the current low resolution of the reference dataset for genetic analyses. As a consequence, the interpretation represents only one hypothesis among several other possibilities, a common methodological problem in bioarchaeological research. For example, the mixed signal measured in the bulk samples of human teeth from Basel-Waisenhaus does not only fit into the range of bioavailable Sr at Basel and in the direct surroundings but also matches $^{87}\text{Sr}/^{86}\text{Sr}$ values measured and modeled over wide areas in Europe.^{72–77} Hence, it cannot be excluded

that mobile individuals originating from areas with similar isotope values would not be visible. In this context, O isotope and aDNA data help reduce the number of possible places of origin: particularly the URA and other regions of eastern France and Central Europe are among the most plausible possibilities.

Both isotope and aDNA data could thus support various contradictory narratives. However, the comparative data generated in the follow-up project from both sides of the Rhine and from contemporaneous as well as later phases will allow us to disentangle further and classify the hitherto ambiguous data. When considered separately, however, this pilot study highlights the limitations of these methods – despite the combination of proxies – in the current state of research and with respect to certain questions, environmental conditions, and sample sizes.

Conclusion

This study again emphasizes the pertinence of interdisciplinary approaches to study Late Antique and Early Medieval societies. Thus, the integration of multi-isotope, aDNA, anthropological, and archaeological analyses on the human remains from Basel-Waisenhaus not only allows for revision of the interpretation of the Basel-Waisenhaus burials but also to gain new insights into the daily organization at the periphery of the Roman Empire. By providing the first evidence of a local community on the northern side of the river Rhine after the latter became again the border of the Western Roman Empire around AD 260 – and even after its fortification led by Valentinian I around AD 374 – this study demonstrates that the loss of the *A. decumates* was not necessarily related to the replacement of the local (Roman) population by immigrated (Alamannic) people. This would support the assumption that during the Late Antiquity and the early fifth century, the population probably mainly remained the same within this area, and only the administrative organization and designations changed.

However, it is essential to stress that neither the archaeological nor the isotopic or genetic records inform about the ethnicity or identity of the buried individuals. This issue has been largely discussed in the last decades, but shifting away from the engrained Roman-German dichotomy is a long ongoing process. Especially with respect to Basel-Waisenhaus, we can argue that the traditional idea of a strict separation between “Romans” living on the southern and immigrated “Alamans” living on the northern bank of the river Rhine needs to be revised. Because of the limitations of the methods and the particularly small sample size, it is not possible to reject the hypothesis that these individuals were descendants from individuals who previously migrated to this area from other parts of Western, Northern or Central Europe. If this were true, the archaeological context would at least suggest a complete integration into the late Roman cultural tradition.

The results of a current project (SNSF project number 100011_208060), including isotope and aDNA data from individuals buried on both riverbanks between the fourth and the seventh century AD in the region of the present-day canton Basel-Stadt, will help better assess the origin of the individuals from Basel-Waisenhaus. It will also enable to update and revise the traditional migration narratives assumed for this border area during this highly dynamic period. Furthermore, the analysis of the genetic background of Basel's Late Antique communities opened new perspectives regarding the impact of the Roman conquest in the first centuries AD on the local population. This hypothesis will be explored in the aforementioned follow-up project as well.

STAR★METHODS

Detailed methods are provided in the online version of this paper and include the following:

- [KEY RESOURCES TABLE](#)
- [RESOURCE AVAILABILITY](#)
 - Lead contact
 - Materials availability
 - Data and code availability
- [EXPERIMENTAL MODEL AND SUBJECT DETAILS](#)
 - Archaeological human samples
 - Ethical statement
- [METHOD DETAILS](#)
 - Environmental suitability analysis
 - Radiocarbon dating

- aDNA analyses
- Strontium and oxygen isotope analyses
- Carbon and nitrogen stable isotope analysis
- **QUANTIFICATION AND STATISTICAL ANALYSIS**

SUPPLEMENTAL INFORMATION

Supplemental information can be found online at <https://doi.org/10.1016/j.isci.2023.107034>.

ACKNOWLEDGMENTS

We would like to thank Yolanda Hecht, Guido Lassau, and Christian Stegmüller (Archäologische Bodenforschung Basel-Stadt) for providing the material and for giving us access to the archives; Nicolas da Silva (Kiel University) for supervising Human population genetic analyses and helping with visualization aspects; Matthew Cooper (National Oceanography Centre, University of Southampton) for mass spectrometry; Moritz Lehmann (University of Basel) for providing access to mass spectrometry facilities; Héctor Martínez-Grau and Ferran Antolin (DAI Berlin) for their advice and support regarding the use of the OxCal software; Joscha Gretzinger (MPI Jena), Ruairidh Macleod (University of Cambridge), and Magdalena Haller (Kiel University) for their support in the interpretation of the genetic data. We are also very grateful to Leah M. Brainerd (University of Cambridge) for her valuable comments on the structure of the manuscript and for proofreading the revised version of the paper. Many thanks to the FFLF – FAG (Fonds zur Förderung von Lehre und Forschung der Freiwilligen Akademischen Gesellschaft, Basel) and the Vindonissa Professorship of the University of Basel for financing parts of this research. MK's research at Kiel was funded by the German Research Foundation and the CRC1266 'Scales of Transformation' under grant number 290391021.

AUTHOR CONTRIBUTIONS

Conceptualization, M.L.C.D., P.A.S., and C.G.; Methodology, M.L.C.D., B.K.K., I.K., M.K., and C.G.; Investigation, M.L.C.D., B.K.K., I.K., M.K., T.K., and C.G.; Formal Analysis, M.L.C.D., M.K., B.K.K., I.H., and C.G.; Resources, N.S.; Writing – Original Draft, M.L.C.D., B.K.K., I.K., M.K., P.A.S., and C.G.; Writing – Review and Editing, M.L.C.D., B.K.K., M.K., T.K., and C.G.; Visualization, M.L.C.D., B.K.K., and M.K.; Supervision, P.A.S. and C.G.; Funding Acquisition, P.A.S.

DECLARATION OF INTERESTS

The authors declare no conflict of interest.

Received: December 14, 2022

Revised: March 23, 2023

Accepted: May 31, 2023

Published: June 8, 2023

REFERENCES

1. Halsall, G. (2014). Two worlds become one: a 'Counter-Intuitive' view of the Roman Empire and 'Germanic' migration. *Ger. Hist.* 32, 515–532. <https://doi.org/10.1093/gerhis/ghu107>.
2. Liebeschuetz, W. (2015). *East and West in Late Antiquity: Invasion, Settlement, Ethnogenesis and Conflicts of Religion* (Brill).
3. W. Pohl, and G. Heydemann, eds. (2013). *Post-Roman Transitions. Christian and Barbarian Identities in the Early Medieval West* (Brepols).
4. Halsall, G. (2007). *Barbarian Migrations and the Roman West* (Cambridge Univ. Press), pp. 376–568.
5. Heather, P.J. (2010). *Empires and Barbarians: The Fall of Rome and the Birth of Europe* (Oxford University Press).
6. Steinacher, R. (2019). Transformation or fall?: perceptions and perspectives on the transition from late antiquity to the early middle ages. In *Archaeology, history and biosciences: Interdisciplinary perspectives*, S. Brather-Walter, ed. (W. De Gruyter), pp. 103–124.
7. Lucy, S. (2000). *The Anglo-Saxon Way of Death: Burial Rites in Early England* (The History Press Ltd).
8. Lucy, S. (2005). Ethnic and cultural identities. In *Archaeology of identity: Approaches to gender, age, status, ethnicity and religion*, M. Díaz-Andreu, S. Lucy, S. Babić, and D.N. Edwards, eds. (Routledge), pp. 89–109.
9. Halsall, G. (2011). Ethnicity and early medieval cemeteries. *AyTM.* 18, 15–27.
10. Brather, S. (2004). *Ethnische Interpretationen in der frühgeschichtlichen Archäologie. Geschichte, Grundlagen und Alternativen*.
11. Heeren, S. (2016). The theory of "Limesfall" and the material culture of the late 3rd century. *Germania* 94, 185–209.
12. Blöck, L. (2019). Die Besiedlung rechts des Rheins. In *Am anderen Flussufer. Die Spätantike beiderseits des südlichen Oberrheins: Sur l'autre rive. L'Antiquité tardive de part et d'autre du Rhin supérieur*

- méridional, G. Kuhnle and E. Wirberlauer, eds., pp. 226–237.
13. Schwarz, P.-A. (2019). Der späntantike Hochrhein-Limes: Zwischenbilanz und Forschungsperspektiven. In *Am anderen Flussufer. Die Spätantike beiderseits des südlichen Oberrheins: Sur l'autre rive. L'Antiquité tardive de part et d'autre du Rhin supérieur méridional*, G. Kuhnle and E. Wirberlauer, eds., pp. 28–43.
 14. Helmig, G. (2005). Basel BS. In *Die Schweiz vom Paläolithikum bis zum frühen Mittelalter VI: Das Frühmittelalter*, R. Windler, R. Marti, U. Niffeler, and L. Steiner, eds. (Schweizerische Gesellschaft für Ur- und Frühgeschichte), pp. 376–378.
 15. Geuenich, D. (2017). Die Alamannia und ihre Grenzen (5. bis 9. Jahrhundert). In *Grenzen, Räume und Identitäten: Der Oberrhein und seine Nachbarregionen von der Antike bis zum Hochmittelalter*, S. Brather and J. Dendorfer, eds. (Jan Thorbecke Verlag), pp. 137–153.
 16. Nuber, H.U. (2014). Der Südwesten in römischer Zeit: Erblasser des Mittelalters? In *Antike im Mittelalter: Fortleben, Nachwirken*, S.B. Wahrnehmung, ed. (J. Thorbecke), pp. 27–49.
 17. Fehr, H. (2013). Bemerkungen zur These einer frühmittelalterlichen Baselromania aus archäologischer Sicht. In *Die Regio Basiliensis von der Antike zum Mittelalter: Land am Rheinknie im Spiegel der Namen = La région de Bâle et les rives du Rhin de l'Antiquité au Moyen Âge : aspects toponymiques et historiques*, A. Greule, W. Müller, and T. Zotz, eds. (Kohlhammer), pp. 161–179.
 18. L. Flutsch, U. Niffeler, and F. Rossi, eds. (2002). *Die Schweiz vom Paläolithikum bis zum frühen Mittelalter: Vom Neandertaler bis zu Karl dem Grossen = La Suisse du Paléolithique à l'aube du Moyen-Age = La Svizzera dal Paleolitico all' Alto Medioevo* (Verl. Schweizer. Ges. für Ur- und Frühgeschichte).
 19. Heising, A. (2017). Kommunikationsräume innerhalb römischer Provinzen: Das Beispiel Germania Superior - eine Provinz mit zwei Gesichtern? In *Grenzen, Räume und Identitäten: Der Oberrhein und seine Nachbarregionen von der Antike bis zum Hochmittelalter*, S. Brather and J. Dendorfer, eds. (Jan Thorbecke Verlag), pp. 199–237.
 20. Baumann, M., Asal, M., and Allemann, M. (2018). Wissenschaftlicher Bericht. Die Spätantike Gräbergruppe Basel-Waisenhaus.: Anthropologische und archäologische Ergebnisse der Ausgrabung 2010/11 - Theodorskirchplatz 7 (Bürgerliches Waisenhaus). Jahresbericht der Archäologischen Bodenforschung Basel-Stadt 2017, 116–139.
 21. Lehmann, S. (2014). Das frühmittelalterliche Gräberfeld von Basel-Gotterbarmweg.
 22. Giesler, U. (1981). Das alamannische Gräberfeld von Basel-Kleinhüningen. Führer zu vor- und frühgeschichtlichen Denkmälern 47, 211–223.
 23. Marti, R. (2018). Mit allem, was dazu gehört. In *50 Jahre - 50 Funde: Archäologie im Kanton Baselland : Begleitpublikation zur Ausstellung "50 Jahre - 50 Funde" im Museum. BL, 8. Juni bis 14 Oktober 2018*, R. Marti and A. Fischer, eds. (Schwabe Verlag).
 24. Depaermentier, M.L.C. (2023). Isotope data in Migration Period Archaeology: critical review and future directions. *Archaeol. Anthropol. Sci.* 15, 42. <https://doi.org/10.1007/s12520-023-01739-y>.
 25. Alt, K.W., Knipper, C., Peters, D., Müller, W., Maurer, A.-F., Kollig, I., Nicklisch, N., Müller, C., Karimnia, S., Brandt, G., et al. (2014). Lombards on the move—an integrative study of the migration period cemetery at Szólád, Hungary. *PLoS One* 9, e110793. <https://doi.org/10.1371/journal.pone.0110793>.
 26. Geary, P., and Veeramah, K. (2016). Mapping European population movement through genomic research. *Medieval Worlds* 4, 65–78. https://doi.org/10.1553/medievalworlds_no4_2016s65.
 27. Pohl, W., Krause, J., Vida, T., and Geary, P. (2021). Integrating genetic, archaeological, and historical perspectives on eastern central Europe, 400–900 AD. *Historical Studies on Central Europe* 1. <https://doi.org/10.47074/HSCSE.2021-1.09>.
 28. Schiffels, S., Haak, W., Paajanen, P., Llamas, B., Popescu, E., Loe, L., Clarke, R., Lyons, A., Mortimer, R., Sayer, D., et al. (2016). Iron age and Anglo-Saxon genomes from East England reveal British migration history. *Nat. Commun.* 7, 10408. <https://doi.org/10.1038/ncomms10408>.
 29. Weale, M.E., Weiss, D.A., Jager, R.F., Bradman, N., and Thomas, M.G. (2002). Y chromosome evidence for Anglo-Saxon mass migration. *Mol. Biol. Evol.* 19, 1008–1021. <https://doi.org/10.1093/oxfordjournals.molbev.a004160>.
 30. Amorim, C.E.G., Vai, S., Posth, C., Modi, A., Koncz, I., Hakenbeck, S., La Rocca, M.C., Mende, B., Bobo, D., Pohl, W., et al. (2018). Understanding 6th-century barbarian social organization and migration through paleogenomics. *Nat. Commun.* 9, 3547. <https://doi.org/10.1038/s41467-018-06024-4>.
 31. Csákyová, V., Gerber, D., Koncz, I., Csiky, G., Mende, B.G., Szeifert, B., Egyed, B., Pamjav, H., Marcsik, A., Molnár, E., et al. (2020). Genetic insights into the social organisation of the Avar period elite in the 7th century AD Carpathian Basin. *Sci. Rep.* 10, 1–14. <https://doi.org/10.1038/s41598-019-57378-8>.
 32. Fernandes, D., Sirak, K., Cheronet, O., Howcroft, R., Čavka, M., Los, D., Burmaz, J., Pinhasi, R., and Novak, M. (2019). Cranial deformation and genetic diversity in three adolescent male individuals from the Great Migration Period from Osijek, eastern Croatia. *PLoS One* 14, e0216366. <https://doi.org/10.1371/journal.pone.0216366>.
 33. Veeramah, K.R., Rott, A., Groß, M., van Dorp, L., López, S., Kirsanow, K., Sell, C., Blöcher, J., Wegmann, D., Link, V., et al. (2018). Population genomic analysis of elongated skulls reveals extensive female-biased immigration in Early Medieval Bavaria. *Proc. Natl. Acad. Sci. USA* 115, 3494–3499. <https://doi.org/10.1073/pnas.1719880115>.
 34. Casas, M.J., Hagelberg, E., Fregel, R., Larruga, J.M., and González, A.M. (2006). Human mitochondrial DNA diversity in an archaeological site in al-Andalus: genetic impact of migrations from North Africa in medieval Spain. *Am. J. Phys. Anthropol.* 131, 539–551. <https://doi.org/10.1002/ajpa.20463>.
 35. Helgason, A., Hickey, E., Goodacre, S., Bosnes, V., Stefánsson, K., Ward, R., and Sykes, B. (2001). mtDNA and the islands of the North Atlantic: estimating the proportions of Norse and Gaelic ancestry. *Am. J. Hum. Genet.* 68, 723–737. <https://doi.org/10.1086/318785>.
 36. Vai, S., Ghirotto, S., Pilli, E., Tassi, F., Lari, M., Rizzi, E., Matas-Lalueza, L., Ramirez, O., Lalueza-Fox, C., Achilli, A., et al. (2015). Genealogical relationships between early medieval and modern inhabitants of piedmont. *PLoS One* 10, e0116801. <https://doi.org/10.1371/journal.pone.0116801>.
 37. Eckardt, H., Müldner, G., and Lewis, M. (2014). People on the move in Roman Britain. *World Archaeol.* 46, 534–550. <https://doi.org/10.1080/00438243.2014.931821>.
 38. Francisci, G., Micarelli, I., Iacumin, P., Castorina, F., Di Vincenzo, F., Di Matteo, M., Giostra, C., Manzi, G., and Tafari, M.A. (2020). Strontium and oxygen isotopes as indicators of Longobards mobility in Italy: an investigation at Povegliano Veronese. *Sci. Rep.* 10, 11678. <https://doi.org/10.1038/s41598-020-67480-x>.
 39. Guede, I., Ortega, L.A., Zuluaga, M.C., Alonso-Olazar, A., Murelaga, X., Pina, M., Gutierrez, F.J., and Iacumin, P. (2017). Isotope analyses to explore diet and mobility in a medieval Muslim population at Tauste (NE Spain). *PLoS One* 12, e0176572. <https://doi.org/10.1371/journal.pone.0176572>.
 40. Knipper, C., Koncz, I., Ódor, J.G., Mende, B.G., Rácz, Z., Kraus, S., van Gysegem, R., Friedrich, R., and Vida, T. (2020). Coalescing traditions-coalescing people: community formation in Pannonia after the decline of the Roman Empire. *PLoS One* 15, e0231760. <https://doi.org/10.1371/journal.pone.0231760>.
 41. Winter-Schuh, C., and Makarewicz, C.A. (2019). Isotopic evidence for changing human mobility patterns after the disintegration of the Western Roman Empire at the Upper Rhine. *Archaeol. Anthropol. Sci.* 11, 2937–2955. <https://doi.org/10.1007/s12520-018-0702-y>.
 42. García-Collado, M.I. (2016). Food consumption patterns and social inequality in an early medieval rural community in the

- centre of the Iberian Peninsula. In *Social complexity in early medieval rural communities: The north-western Iberia archaeological record*, J.A. Quirós Castillo, ed. (Archaeopress Archaeology), pp. 59–78.
43. Hakenbeck, S.E., Evans, J., Chapman, H., and Fóthi, E. (2017). Practising pastoralism in an agricultural environment: an isotopic analysis of the impact of the Hunnic incursions on Pannonian populations. *PLoS One* 12, e0173079. <https://doi.org/10.1371/journal.pone.0173079>.
 44. Iacumin, P., Galli, E., Cavalli, F., and Cecere, L. (2014). C4 -consumers in southern Europe: the case of Friuli V.G. (NE-Italy) during early and central Middle Ages. *Am. J. Phys. Anthropol.* 154, 561–574. <https://doi.org/10.1002/ajpa.22553>.
 45. Leggett, S. (2021). 'Tell Me what You Eat, and I Will Tell You Who You Are': A Multi-Tissue and Multi-Scalar Isotopic Study of Diet and Mobility in Early Medieval England and its European Neighbours. (Univ. Diss., University of Cambridge).
 46. Leggett, S. (2021). Migration and cultural integration in the early medieval cemetery of Finglesham, Kent, through stable isotopes. *Archaeol. Anthropol. Sci.* 13, 171. <https://doi.org/10.1007/s12520-021-01429-7>.
 47. Lightfoot, E., Šlaus, M., and O'Connell, T.C. (2012). Changing cultures, changing cuisines: cultural transitions and dietary change in Iron age, Roman, and early medieval Croatia. *Am. J. Phys. Anthropol.* 148, 543–556. <https://doi.org/10.1002/ajpa.22070>.
 48. Fuller, B.T., Márquez-Grant, N., and Richards, M.P. (2010). Investigation of diachronic dietary patterns on the islands of Ibiza and formentera, Spain: evidence from carbon and nitrogen stable isotope ratio analysis. *Am. J. Phys. Anthropol.* 143, 512–522. <https://doi.org/10.1002/ajpa.21334>.
 49. Hakenbeck, S., McManus, E., Geisler, H., Grupe, G., and O'Connell, T. (2010). Diet and mobility in Early Medieval Bavaria: a study of carbon and nitrogen stable isotopes. *Am. J. Phys. Anthropol.* 143, 235–249. <https://doi.org/10.1002/ajpa.21309>.
 50. Bentley, R., Price, T., and Stephan, E. (2004). Determining the 'local' $^{87}\text{Sr}/^{86}\text{Sr}$ range for archaeological skeletons: a case study from Neolithic Europe. *J. Archaeol. Sci.* 31, 365–375. <https://doi.org/10.1016/j.jas.2003.09.003>.
 51. Alexander Bentley, R. (2006). Strontium isotopes from the Earth to the archaeological skeleton: a review. *J. Archaeol. Method Theory* 13, 135–187. <https://doi.org/10.1007/s10816-006-9009-x>.
 52. Price, D.T., Frei, K.M., Tiesler, V., and Gestsdóttir, H. (2012). Isotopes and mobility. Case studies with large samples. In *Population Dynamics in Prehistory and Early History: New Approaches by Using Stable Isotopes and Genetic*, E. Kaiser, J. Burger, and W. Schier, eds. (De Gruyter), pp. 311–321.
 53. van Klinken, G.J., Richards, M.P., and Hedges, R.E.M. (2000). An overview of causes for stable isotopic variations in past European human populations. *Environmental, ecophysiological, and cultural effects*. In *Biogeochemical approaches to paleodietary analysis: Advances in archaeological and museum science*, S.H. Ambrose and M.A. Katzenberg, eds., pp. 39–63.
 54. Chenery, C.A., Pashley, V., Lamb, A.L., Sloane, H.J., and Evans, J.A. (2012). The oxygen isotope relationship between the phosphate and structural carbonate fractions of human bioapatite. *Rapid Commun. Mass Spectrom.* 26, 309–319. <https://doi.org/10.1002/rcm.5331>.
 55. D'Angela, D., and Longinelli, A. (1990). Oxygen isotopes in living mammal's bone phosphate: further results. *Chem. Geol.* 86, 75–82.
 56. Pederzani, S., and Britton, K. (2019). Oxygen isotopes in bioarchaeology: principles and applications, challenges and opportunities. *Earth Sci. Rev.* 188, 77–107. <https://doi.org/10.1016/j.earscirev.2018.11.005>.
 57. Brönnimann, D., Knipper, C., Pichler, S.L., Röder, B., Rissanen, H., Stopp, B., Rosner, M., Blank, M., Warnberg, O., Alt, K.W., et al. (2018). The lay of land: strontium isotope variability in the dietary catchment of the Late Iron Age proto-urban settlement of Basel-Gasfabrik, Switzerland. *J. Archaeol. Sci.: Reports* 17, 279–292. <https://doi.org/10.1016/j.jasrep.2017.11.009>.
 58. Knipper, C., Pichler, S.L., Brönnimann, D., Rissanen, H., Rosner, M., Spichtig, N., Stopp, B., Rentzel, P., Röder, B., Schibler, J., et al. (2018). A knot in a network: residential mobility at the Late Iron Age proto-urban centre of Basel-Gasfabrik (Switzerland) revealed by isotope analyses. *J. Archaeol. Sci.: Reports* 17, 735–753. <https://doi.org/10.1016/j.jasrep.2017.12.001>.
 59. Kempf, M., and Depaermentier, M.L.C. (2023). Scales of transformations - modelling settlement and land-use dynamics in late Antique and early medieval Basel, Switzerland. *PLoS One* 18, e0280321. <https://doi.org/10.1371/journal.pone.0280321>.
 60. Ramsey, C.B. (2021). *OxCal*.
 61. Reimer, P.J., Austin, W.E.N., Bard, E., Bayliss, A., Blackwell, P.G., Bronk Ramsey, C., Butzin, M., Cheng, H., Edwards, R.L., Friedrich, M., et al. (2020). The IntCal20 northern hemisphere radiocarbon age calibration curve (0–55 cal kBP). *Radiocarbon* 62, 725–757. <https://doi.org/10.1017/RDC.2020.41>.
 62. Ramsey, C.B. (2017). Methods for summarizing radiocarbon datasets. *Radiocarbon* 59, 1809–1833. <https://doi.org/10.1017/RDC.2017.108>.
 63. Wild, E., Golser, R., Hille, P., Kutschera, W., Priller, A., Puchegger, S., Rom, W., Steier, P., and Vycudilik, W. (1997). First 14 C results from archaeological and forensic studies at the vienna environmental research accelerator. *Radiocarbon* 40, 273–281. <https://doi.org/10.1017/S0033822200018142>.
 64. Wild, E., Arlamovsky, K., Golser, R., Kutschera, W., Priller, A., Puchegger, S., Rom, W., Steier, P., and Vycudilik, W. (2000). 14C dating with the bomb peak: an application to forensic medicine. *Nucl. Instrum. Methods Phys. Res. Sect. B Beam Interact. Mater. Atoms* 172, 944–950. [https://doi.org/10.1016/S0168-583X\(00\)00227-5](https://doi.org/10.1016/S0168-583X(00)00227-5).
 65. Hajdas, I., Ascough, P., Garnett, M.H., Fallon, S.J., Pearson, C.L., Quarta, G., Spalding, K.L., Yamaguchi, H., and Yoneda, M. (2021). Radiocarbon dating. *Nat. Rev. Methods Primers* 1, 62. <https://doi.org/10.1038/s43586-021-00058-7>.
 66. Bentley, R.A., and Knipper, C. (2005). Geographical patterns in biologically available strontium, carbon and oxygen isotope signatures in prehistoric SW Germany. *Archaeometry* 47, 629–644. <https://doi.org/10.1111/j.1475-4754.2005.00223.x>.
 67. Schuh, C., and Makarewicz, C.A. (2016). Tracing residential mobility during the Merovingian period: an isotopic analysis of human remains from the Upper Rhine Valley, Germany. *Am. J. Phys. Anthropol.* 161, 155–169. <https://doi.org/10.1002/ajpa.23017>.
 68. Oelze, V.M., Nehlich, O., and Richards, M.P. (2012). There's no place like home: No isotopic evidence for mobility at the Early Bronze Age cemetery of Singen, Germany. *Archaeometry* 54, 752–778. <https://doi.org/10.1111/j.1475-4754.2011.00644.x>.
 69. Sjögren, K.G., Price, T.D., and Kristiansen, K. (2016). Diet and mobility in the corded ware of central Europe. *PLoS One* 11, e0155083. <https://doi.org/10.1371/journal.pone.0155083>.
 70. Bickle, P., Arbogast, R.-M., Bentley, R.A., Fibiger, L., Hamilton, J., Hedges, R.E.M., and Whittle, A. (2013). Alsace. In *The first farmers of central Europe: Diversity in LBK lifeways*, P. Bickle and A. Whittle, eds. (Oxbow Books and the David Brown Book Company), pp. 291–342.
 71. Bentley, R.A., Bickle, P., Francken, M., Gerling, C., Hamilton, J., Hedges, R.E.M., Stephan, E., Wahl, J., and Whittle, A. (2013). Baden-württemberg. In *The first farmers of central Europe: Diversity in LBK lifeways*, P. Bickle and A. Whittle, eds. (Oxbow Books and the David Brown Book Company), pp. 251–290.
 72. Depaermentier, M.L.C., Kempf, M., Bánffy, E., and Alt, K.W. (2021). Modelling a scale-based strontium isotope baseline for Hungary. *J. Archaeol. Sci.* 135, 1–16. <https://doi.org/10.1016/j.jas.2021.105489>.
 73. Bataille, C.P., von Holstein, I.C.C., Laffoon, J.E., Willmes, M., Liu, X.-M., and Davies, G.R. (2018). A bioavailable strontium isoscape for

- Western Europe: a machine learning approach. *PLoS One* 13, e0197386. <https://doi.org/10.1371/journal.pone.0197386>.
74. Willmes, M., Bataille, C.P., James, H.F., Moffat, I., McMorrow, L., Kinsley, L., Armstrong, R.A., Eggins, S., and Grün, R. (2018). Mapping of bioavailable strontium isotope ratios in France for archaeological provenance studies. *Appl. Geochem.* 90, 75–86. <https://doi.org/10.1016/j.apgeochem.2017.12.025>.
 75. Voerkelius, S., Lorenz, G.D., Rummel, S., Quénel, C.R., Heiss, G., Baxter, M., Brach-Papa, C., Deters-Iltzelsberger, P., Hoelzl, S., Hoogewerff, J., et al. (2010). Strontium isotopic signatures of natural mineral waters, the reference to a simple geological map and its potential for authentication of food. *Food Chem.* 118, 933–940. <https://doi.org/10.1016/j.foodchem.2009.04.125>.
 76. Díaz-del-Río, P., Uriarte, A., Becerra, P., Pérez-Villa, A., Vicent, J.M., and Díaz-Zorita, M. (2022). Paleomobility in Iberia: 12 years of strontium isotope research. *J. Archaeol. Sci.: Reports* 46, 103653. <https://doi.org/10.1016/j.jasrep.2022.103653>.
 77. P. Bickle, and A. Whittle, eds. (2013). *The first farmers of central Europe: Diversity in LBK lifeways (Oxbow Books and the David Brown Book Company)*.
 78. Coplen, T.B., Kendall, C., and Hopple, J. (1983). Comparison of stable isotope reference samples. *Nature* 302, 236–238. <https://doi.org/10.1038/302236a0>.
 79. Iacumin, P., Bocherens, H., Mariotti, A., and Longinelli, A. (1996). Oxygen isotope analyses of co-existing carbonate and phosphate in biogenic apatite: a way to monitor diagenetic alteration of bone phosphate? *Earth Planet Sci. Lett.* 142, 1–6. [https://doi.org/10.1016/0012-821X\(96\)00093-3](https://doi.org/10.1016/0012-821X(96)00093-3).
 80. Knipper, C., Pichler, S.L., Rissanen, H., Stopp, B., Kühn, M., Spichtig, N., Röder, B., Schibler, J., Lassau, G., and Alt, K.W. (2017). What is on the menu in a Celtic town? Iron Age diet reconstructed at Basel-Gasfabrik, Switzerland. *Archaeol. Anthropol. Sci.* 9, 1307–1326. <https://doi.org/10.1007/s12520-016-0362-8>.
 81. Grau-Sologestoa, I., Deschler-Erb, S., and Gerling, C. (submitted). Livestock management during times of change. Exploring the relationship between animal size and diet from Roman to early medieval Augusta Raurica (Switzerland). *Archaeological and Anthropological Sciences*
 82. Ambrose, S.H. (1990). Preparation and characterization of bone and tooth collagen from isotopic analysis. *J. Archaeol. Sci.* 17, 431–451.
 83. DeNiro, M.J. (1985). Postmortem preservation and alteration of in vivo bone collagen isotope ratios in relation to palaeodietary reconstruction. *Nature* 317, 806–809. <https://doi.org/10.1038/317806a0>.
 84. Britton, K., Fuller, B.T., Tütken, T., Mays, S., and Richards, M.P. (2015). Oxygen isotope analysis of human bone phosphate evidences weaning age in archaeological populations. *Am. J. Phys. Anthropol.* 157, 226–241. <https://doi.org/10.1002/ajpa.22704>.
 85. Büntgen, U., Myglan, V.S., Ljungqvist, F.C., McCormick, M., Di Cosmo, N., Sigl, M., Jungclauss, J., Wagner, S., Krusic, P.J., Esper, J., et al. (2016). Cooling and societal change during the late Antique little ice age from 536 to around 660 AD. *Nat. Geosci.* 9, 1–7. <https://doi.org/10.1038/ngeo2652>.
 86. Lightfoot, E., Šlaus, M., Šikanjić, P.R., and O'Connell, T.C. (2015). Metals and millets: Bronze and Iron Age diet in inland and coastal Croatia seen through stable isotope analysis. *Archaeol. Anthropol. Sci.* 7, 375–386.
 87. Carroll, G., Inskip, S., and Waters-Rist, A. (2018). Pathophysiological stable isotope fractionation: assessing the impact of anemia on enamel apatite $\delta^{18}\text{O}$ and $\delta^{13}\text{C}$ values and bone collagen $\delta^{15}\text{N}$ and $\delta^{13}\text{C}$ values. *BI 2*, 117–146. <https://doi.org/10.5744/bi.2018.1021>.
 88. Linderholm, A., and Kjellström, A. (2011). Stable isotope analysis of a medieval skeletal sample indicative of systemic disease from Sigtuna Sweden. *J. Archaeol. Sci.* 38, 925–933. <https://doi.org/10.1016/j.jas.2010.11.022>.
 89. Scorrano, G., Brilli, M., Martínez-Labarga, C., Giustini, F., Pacciani, E., Chilleri, F., Scaldaferrri, F., Gasbarrini, A., Gasbarrini, G., and Rickards, O. (2014). Palaeodiet reconstruction in a woman with probable celiac disease: a stable isotope analysis of bone remains from the archaeological site of Cosa (Italy). *Am. J. Phys. Anthropol.* 154, 349–356. <https://doi.org/10.1002/ajpa.22517>.
 90. Armelagos, G.J., Sirak, K., Werkema, T., and Turner, B.L. (2014). Analysis of nutritional disease in prehistory: the search for scurvy in antiquity and today. *Int. J. Paleopathol.* 5, 9–17. <https://doi.org/10.1016/j.ijpp.2013.09.007>.
 91. Garland, C., Reitsema, L., Larsen, C.S., and Thomas, D.H. (2018). Early life stress at mission Santa Catalina de Guale: an integrative analysis of enamel defects and Dentin incremental isotope variation in malnutrition. *BI 2*, 75–94. <https://doi.org/10.5744/bi.2018.1019>.
 92. Gismondi, A., Baldoni, M., Gnes, M., Scorrano, G., D'Agostino, A., Di Marco, G., Calabria, G., Petrucci, M., Müldner, G., Von Tersch, M., et al. (2020). A multidisciplinary approach for investigating dietary and medicinal habits of the Medieval population of Santa Severa (7th–15th centuries, Rome, Italy). *PLoS One* 15, e0227433. <https://doi.org/10.1371/journal.pone.0227433>.
 93. Reitsema, L.J. (2013). Beyond diet reconstruction: stable isotope applications to human physiology, health, and nutrition. *Am. J. Hum. Biol.* 25, 445–456. <https://doi.org/10.1002/ajhb.22398>.
 94. Reitsema, L., and Holder, S. (2018). Stable isotope analysis and the study of human stress, disease, and nutrition. *BI 2*, 63–74. <https://doi.org/10.5744/bi.2018.1018>.
 95. Scorrano, G. (2018). The stable isotope method in human paleopathology and nutritional stress analysis. *Archaeology & Anthropology: Open Access* 1. <https://doi.org/10.31031/AAOA.2018.01.000523>.
 96. Scorrano, G., Baldoni, M., Brilli, M., Rolfo, M.F., Fornaciari, G., Rickards, O., and Martínez-Labarga, C. (2019). Effect of neolithic transition on an Italian community: Mora Cavorso (Jenne, Rome). *Archaeol. Anthropol. Sci.* 11, 1443–1459. <https://doi.org/10.1007/s12520-018-0615-9>.
 97. Marcellinus, A. (1968–1971). *Römische Geschichte: [30,3,1–2]*.
 98. Theodosius II (1923–1926). *Codex Theodosianus I–II: Recognovit Paulus Krueger*.
 99. *The Theodosian Code and Novels and the Sirmundian Constitutions: A Translation with Commentary, Glossary and Bibliography* (1952 (Princeton University Press)).
 100. Asal, M. (2017). *Basilia – Das Spätantike Basel: Band A (Archäologische Bodenforschung des Kantons Basel-Stadt)*.
 101. Bruner, S. (2014). *Eine spätrömische Nekropole westlich des Castrum Rauracense: Das Gräberfeld Kaiseraugst-Höll. Jahresberichte aus Augst und Kaiseraugst* 35, 241–331.
 102. Perréard Lopreno, G. (2005). Die Bevölkerung des Frühmittelalters: Beiträge der Paläoanthropologie. In *Die Schweiz vom Paläolithikum bis zum frühen Mittelalter VI: Das Frühmittelalter*, R. Windler, R. Marti, U. Niffeler, and L. Steiner, eds. (Schweizerische Gesellschaft für Ur- und Frühgeschichte), pp. 173–180.
 103. Steiner, L., and Menna, F. (2000). *La nécropole du Pré de la Cure à Yverdon-les-Bains (IVe–VIIe s. ap. J.-C.)*.
 104. Høilund Nielsen, K. (2011). Animal style and elite communication in the later 5th and 6th centuries. In *Weibliche Eliten in der Frühgeschichte: = Female Elites in Protohistoric Europe*, D. Quast, ed. (Verlag des Römisch-Germanischen Zentralmuseums), pp. 361–376.
 105. Martin, M. (1997). Zwischen den Fronten: Alamannen im Römischen Heer. In *Die Alamannen: Ausstellungskatalog, Archäologisches Landesmuseum Baden-Württemberg* (Theiss), pp. 119–124.
 106. Mathisen, R.W. (2019). The end of the western Roman Empire in the fifth century CE: Barbarian Auxiliaries, independent military contractors and civil wars. In *The Fifth Century: Age of transformation: proceedings of the 12th biennial shifting frontiers in late antiquity conference*, N. Lenski and J.W. Drijvers, eds. (Edipuglia), pp. 137–156.

107. Effros, B. (2002). *Caring for Body and Soul: Burial and the Afterlife in the Merovingian World* (Pennsylvania State University Press).
108. Effros, B. (2003). *Merovingian Mortuary Archaeology and the Making of the Early Middle Ages* (University of California Press).
109. Halsall, G. (2010). *Cemeteries and Society in Merovingian Gaul: Selected Studies in History and Archaeology, 1992-2009* (Brill).
110. Brownlee, E. (2021). Connectivity and funerary change in early medieval Europe. *Antiquity* 95, 142–159. <https://doi.org/10.15184/aqy.2020.153>.
111. Fehr, H. (2010). Germanen und Romanen im Merowingerreich: Frühgeschichtliche Archäologie zwischen Wissenschaft und Zeitgeschehen (Walter De Gruyter).
112. Maran, J. (2019). Not ‘cultures’ but culture! The need for a transcultural perspective in archaeology. In *Engaging Transculturality, L. Abu-Er-Rub, C. Brosius, S. Meurer, D. Panagiotopoulos, and S. Richter, eds.* (Routledge), pp. 52–64.
113. Martin, T.F. (2020). Casting the net wider: network approaches to Artefact variation in post-Roman Europe. *J. Archaeol. Method Theory* 27, 861–886. <https://doi.org/10.1007/s10816-019-09441-x>.
114. Alt, K.W., Müller, C., and Held, P. (2018). Ernährungsrekonstruktion anhand stabiler Isotope von Kohlenstoff und Stickstoff an frühmittelalterlichen Bestattungen der Gräberfelder von Tauberbischofsheim-Dittigheim und Szólád. In *Lebenswelten zwischen Archäologie und Geschichte: Festschrift für Falko Daim zu seinem 65. Geburtstag*, J. Drauschke, E. Kislinger, K. Kühnreiter, T. Kühnreiter, G. Scharrer-Liska, and T. Vida, eds. (Verlag des Römisch-Germanischen Zentralmuseums), pp. 869–885.
115. Czermak, A., Ledderose, A., Strott, N., Meier, T., and Grupe, G. (2006). Social structures and social relations - an archaeological and anthropological Examination of three early medieval separate burial sites in Bavaria. *Anthropol. Anz.* 64, 297–310.
116. Strott, N., Czermak, A., and Grupe, G. (2008). Are there biological correlates to social stratification? Investigation of early medieval separated burial grounds in Bavaria. *Documenta Archaeobiologiae* 5.
117. Knipper, C., Peters, D., Meyer, C., Maurer, A.-F., Muhl, A., Schöne, B.R., and Alt, K.W. (2013). Dietary reconstruction in Migration Period Central Germany: a carbon and nitrogen isotope study. *Archaeol. Anthropol. Sci.* 5, 17–35. <https://doi.org/10.1007/s12520-012-0106-3>.
118. Czermak, A. (2019). Diet reconstruction based on C/N stable isotope analysis: what can it contribute to Address questions on cultural change? In *Archaeology, history and biosciences: Interdisciplinary perspectives*, S. Brather-Walter, ed. (W. De Gruyter), pp. 181–197.
119. Schutkowski, H., Herrmann, B., Wiedemann, F., Bocherens, H., and Grupe, G. (1999). Diet, status and Decomposition at Weingarten: trace element and isotope analyses on early mediaeval skeletal material. *J. Archaeol. Sci.* 26, 675–685.
120. Plecerová, A., Kaupová Drtikolová, S., Šmerda, J., Stloukal, M., and Velemínský, P. (2020). Dietary reconstruction of the Moravian Lombard population (Kyjov, 5th–6th centuries AD, Czech Republic) through stable isotope analysis ($\delta^{13}C$, $\delta^{15}N$). *J. Archaeol. Sci.*: Reports 29, 102062. <https://doi.org/10.1016/j.jasrep.2019.102062>.
121. Leggett, S. (2022). A hierarchical meta-analytical approach to western European dietary transitions in the first Millennium AD. *Eur. J. Archaeol.* 25, 523–543. <https://doi.org/10.1017/eea.2022.23>.
122. Knipper, C., Mitnik, A., Massy, K., Kociumaka, C., Kucukkalipci, I., Maus, M., Wittenborn, F., Metz, S.E., Staskiewicz, A., Krause, J., and Stockhammer, P.W. (2017). Female exogamy and gene pool diversification at the transition from the final neolithic to the early Bronze age in central Europe. *Proc. Natl. Acad. Sci. USA* 114, 10083–10088. <https://doi.org/10.1073/pnas.1706355114>.
123. Wilhelmson, H., and Ahlström, T. (2015). Iron Age migration on the island of Öland: Apportionment of strontium by means of Bayesian mixing analysis. *J. Archaeol. Sci.* 64, 30–45. <https://doi.org/10.1016/j.jas.2015.09.007>.
124. Böhme, H.W. (1974). *Germanische Grabfunde des 4. bis 5. Jahrhunderts zwischen unterer Elbe und Loire: Studien zur Chronologie und Bevölkerungsgeschichte* (Beck).
125. Nuber, H.U. (2005). Staatskrise im 3. Jahrhundert. Die Aufgabe der rechtsrheinischen Gebiete. In *Imperium Romanum: Roms Provinzen an Neckar, Rhein und Donau*, S. Schmidt, ed. (Theiss; Archäologisches Landesmuseum Baden-Württemberg), pp. 442–451.
126. Margreiter, P. (2019). Bemerkungen zu den frühen Alamannen. In *Am anderen Flussufer. Die Spätantike beiderseits des südlichen Oberrheins: Sur l'autre rive. L'Antiquité tardive de part et d'autre du Rhin supérieur méridional*, G. Kuhle and E. Wirberlauer, eds., pp. 44–51.
127. Steuer, H. (2017). Die Formierung der "Alamannen" in der Spätantike. In *Grenzen, Räume und Identitäten: Der Oberrhein und seine Nachbarregionen von der Antike bis zum Hochmittelalter*, S. Brather and J. Dendorfer, eds. (Jan Thorbecke Verlag), pp. 239–286.
128. Li, H., and Durbin, R. (2010). Fast and accurate long-read alignment with Burrows-Wheeler transform. *Bioinformatics* 26, 589–595. <https://doi.org/10.1093/bioinformatics/btp698>.
129. Neukamm, J., Peltzer, A., and Nieselt, K. (2021). DamageProfiler: fast damage pattern calculation for ancient DNA. *Bioinformatics*. <https://doi.org/10.1093/bioinformatics/btab190>.
130. Renaud, G., Slon, V., Duggan, A.T., and Kelso, J. (2015). Schmutzi: estimation of contamination and endogenous mitochondrial consensus calling for ancient DNA. *Genome Biol.* 16, 224. <https://doi.org/10.1186/s13059-015-0776-0>.
131. Korneliussen, T.S., Albrechtsen, A., and Nielsen, R. (2014). ANGSD: analysis of next generation sequencing data. *BMC Bioinform.* 15, 356. <https://doi.org/10.1186/s12859-014-0356-4>.
132. Jun, G., Wing, M.K., Abecasis, G.R., and Kang, H.M. (2015). An efficient and scalable analysis framework for variant extraction and refinement from population-scale DNA sequence data. *Genome Res.* 25, 918–925. <https://doi.org/10.1101/gr.176552.114>.
133. Weissensteiner, H., Pacher, D., Kloss-Brandstätter, A., Forer, L., Specht, G., Bandelt, H.-J., Kronenberg, F., Salas, A., and Schönherr, S. (2016). HaploGrep 2: mitochondrial haplogroup classification in the era of high-throughput sequencing. *Nucleic Acids Res.* 44, W58–W63. <https://doi.org/10.1093/nar/gkw233>.
134. Poznik, G.D., Speed, N., Hübner, A., Lopker, B. (2016). Identifying Y-chromosome haplogroups in arbitrarily large samples of sequenced or genotyped men. Preprint at bioRxiv. <https://doi.org/10.1101/088716>.
135. Patterson, N., Price, A.L., and Reich, D. (2006). Population structure and eigenanalysis. *PLoS Genet.* 2, e190. <https://doi.org/10.1371/journal.pgen.0020190>.
136. Patterson, N., Moorjani, P., Luo, Y., Mallick, S., Rohland, N., Zhan, Y., Genschoreck, T., Webster, T., and Reich, D. (2012). Ancient admixture in human history. *Genetics* 192, 1065–1093. <https://doi.org/10.1534/genetics.112.145037>.
137. Alexander, D.H., Novembre, J., and Lange, K. (2009). Fast model-based estimation of ancestry in unrelated individuals. *Genome Res.* 19, 1655–1664. <https://doi.org/10.1101/gr.094052.109>.
138. Monroy Kuhn, J.M., Jakobsson, M., and Günther, T. (2018). Estimating genetic kin relationships in prehistoric populations. *PLoS One* 13, e0195491. <https://doi.org/10.1371/journal.pone.0195491>.
139. Knitter, D., Brozio, J.P., Dörfler, W., Duttmann, R., Feeser, I., Hamer, W., Kirleis, W., Müller, J., and Nakoinz, O. (2019). Transforming landscapes: modeling land-use patterns of environmental borderlands. *Holocene* 29, 1572–1586. <https://doi.org/10.1177/0959683619857233>.
140. Laabs, J., and Knitter, D. (2021). How much is enough? First steps to a social Ecology of the Pergamon microregion. *Land* 10, 479. <https://doi.org/10.3390/land10050479>.
141. Nakoinz, O. (2019). *Zentralität. Theorie, Methoden und Fallbeispiele zur Analyse zentraler Orte* (Humboldt-Universität zu Berlin).

142. Hajdas, I., Bonani, G., Furrer, H., Mäder, A., and Schoch, W. (2007). Radiocarbon chronology of the mammoth site at Niederweningen, Switzerland: results from dating bones, teeth, wood, and peat. *Quat. Int.* 164–165, 98–105. <https://doi.org/10.1016/j.quaint.2006.10.007>.
143. Brock, F., Higham, T., and Ramsey, C.B. (2010). Pre-screening techniques for identification of samples suitable for radiocarbon dating of poorly preserved bones. *J. Archaeol. Sci.* 37, 855–865. <https://doi.org/10.1016/j.jas.2009.11.015>.
144. Hajdas, I., Michczyński, A., Bonani, G., Wacker, L., and Furrer, H. (2009). Dating bones near the limit of the radiocarbon dating method: study case mammoth from Niederweningen, ZH Switzerland. *Radiocarbon* 51, 675–680. <https://doi.org/10.1017/S0033822200056010>.
145. Pawelczyk, F., Hajdas, I., Sadykov, T., Blochin, J., and Caspari, G. (2022). Comparing analysis of pretreatment methods of wood and bone materials for the chronology of peripheral burials at Tunnug 1, Tuva Republic, Russia. *Radiocarbon* 64, 171–186. <https://doi.org/10.1017/RDC.2021.100>.
146. Némec, M., Wacker, L., Hajdas, I., and Gäggeler, H. (2010). Alternative methods for cellulose preparation for AMS measurement. *Radiocarbon* 52, 1358–1370. <https://doi.org/10.1017/S0033822200046440>.
147. Synal, H.-A., Stocker, M., and Suter, M. (2007). MICADAS: a new compact radiocarbon AMS system. *Nucl. Instrum. Methods Phys. Res. Sect. B Beam Interact. Mater. Atoms* 259, 7–13. <https://doi.org/10.1016/j.nimb.2007.01.138>.
148. Krause-Kyora, B., Nutsua, M., Boehme, L., Pierini, F., Pedersen, D.D., Kornell, S.-C., Drichel, D., Bonazzi, M., Möbus, L., Tarp, P., et al. (2018). Ancient DNA study reveals HLA susceptibility locus for leprosy in medieval Europeans. *Nat. Commun.* 9, 1569. <https://doi.org/10.1038/s41467-018-03857-x>.
149. Cooper, A., and Poinar, H.N. (2000). Ancient DNA: do it right or not at all. *Science* 289, 1139. <https://doi.org/10.1126/science.289.5482.1139b>.
150. Rohland, N., Harney, E., Mallick, S., Nordenfelt, S., and Reich, D. (2015). Partial uracil-DNA-glycosylase treatment for screening of ancient DNA. *Philos. Trans. R. Soc. Lond. B Biol. Sci.* 370, 20130624. <https://doi.org/10.1098/rstb.2013.0624>.
151. Immel, A., Pierini, F., Rinne, C., Meadows, J., Barquera, R., Szolek, A., Susat, J., Böhme, L., Dose, J., Bonczarowska, J., et al. (2021). Genome-wide study of a Neolithic Wartberg grave community reveals distinct HLA variation and hunter-gatherer ancestry. *Commun. Biol.* 4, 113. <https://doi.org/10.1038/s42003-020-01627-4>.
152. Li, H., and Durbin, R. (2009). Fast and accurate short read alignment with Burrows-Wheeler transform. *Bioinformatics* 25, 1754–1760. <https://doi.org/10.1093/bioinformatics/btp324>.
153. Peltzer, A., Jäger, G., Herbig, A., Seitz, A., Knip, C., Krause, J., and Nieselt, K. (2016). EAGER: efficient ancient genome reconstruction. *Genome Biol.* 17, 60. <https://doi.org/10.1186/s13059-016-0918-z>.
154. Neukamm, J., Pfrengle, S., Molak, M., Seitz, A., Francken, M., Eppenberger, P., Avanzi, C., Reiter, E., Urban, C., Welte, B., et al. (2020). 2000-year-old pathogen genomes reconstructed from metagenomic analysis of Egyptian mummified individuals. *BMC Biol.* 18, 108. <https://doi.org/10.1186/s12915-020-00839-8>.
155. Haak, W., Lazaridis, I., Patterson, N., Rohland, N., Mallick, S., Llamas, B., Brandt, G., Nordenfelt, S., Harney, E., Stewardson, K., et al. (2015). Massive migration from the steppe was a source for Indo-European languages in Europe. *Nature* 522, 207–211. <https://doi.org/10.1038/nature14317>.
156. Lazaridis, I., Patterson, N., Mittnik, A., Renaud, G., Mallick, S., Kirsanow, K., Sudmant, P.H., Schraiber, J.G., Castellano, S., Lipson, M., et al. (2014). Ancient human genomes suggest three ancestral populations for present-day Europeans. *Nature* 513, 409–413. <https://doi.org/10.1038/nature13673>.
157. Mathieson, I., Lazaridis, I., Rohland, N., Mallick, S., Patterson, N., Roodenberg, S.A., Harney, E., Stewardson, K., Fernandes, D., Novak, M., et al. (2015). Genome-wide patterns of selection in 230 ancient Eurasians. *Nature* 528, 499–503. <https://doi.org/10.1038/nature16152>.
158. Skoglund, P., Storå, J., Götherström, A., and Jakobsson, M. (2013). Accurate sex identification of ancient human remains using DNA shotgun sequencing. *J. Archaeol. Sci.* 40, 4477–4482. <https://doi.org/10.1016/j.jas.2013.07.004>.
159. Gerling, C. (2015). *Prehistoric Mobility and Diet in Western Eurasia Steppes 3500 to 300 BC: An Isotopic Approach (De Gruyter)*.
160. Milella, M., Gerling, C., Doppler, T., Kuhn, T., Cooper, M., Mariotti, V., Belcastro, M.G., Ponce de León, M.S., and Zollikofer, C.P. (2019). Different in death: different in life? Diet and mobility correlates of irregular burials in a Roman necropolis from Bologna (Northern Italy, 1st–4th century CE). *J. Archaeol. Sci.: Reports* 27, 101926. <https://doi.org/10.1016/j.jasrep.2019.101926>.
161. Longin, R. (1971). New method of collagen extraction for radiocarbon dating. *Nature* 230, 241–242. <https://doi.org/10.1038/230241a0>.
162. Knipper, C., Reinhold, S., Gresky, J., Berezina, N., Gerling, C., Pichler, S.L., Buzhilova, A.P., Kantorovich, A.R., Maslov, V.E., Petrenko, V.G., et al. (2020). Diet and subsistence in Bronze Age pastoral communities from the southern Russian steppes and the North Caucasus. *PLoS One* 15, e0239861. <https://doi.org/10.1371/journal.pone.0239861>.

STAR★METHODS

KEY RESOURCES TABLE

REAGENT or RESOURCE	SOURCE	IDENTIFIER
Chemicals, peptides, and recombinant proteins		
Bleach (Danklorix)	Colgate-Palmolive	
Nitric acid ROTIPURAN® Supra,69%	Roth AG	CAS No. 7697-37-2
Hydrochloric acid 0.5mol/l	Roth AG	CAS No. 7647-01-0
Sodium hydroxide 0.1 mol/l	Roth AG	CAS No. 1310-73-2
Deposited data		
Raw and analysed data	This study	Table S1
Genetic kinship data	This study	Table S2
Raw data (aDNA)	European Nucleotide Archive (ENA)	ENA: PRJEB60689
Reference dataset (aDNA)	David Reich Lab (see AADR)	https://reich.hms.harvard.edu/allen-ancient-dna-resource-aadr-downloadable-genotypes-present-day-and-ancient-dna-data
Baseline strontium and oxygen isotope data	Brönnimann et al. 2018; Knipper et al. 2018 ^{57,58}	https://doi.org/10.1016/j.jasrep.2017.12.001 ; https://doi.org/10.1016/j.jasrep.2017.11.009
Baseline carbon and nitrogen isotope data	Knipper et al. ^{80,122} ; Grau-Sologestoa et al. in review ⁹²	https://doi.org/10.1007/s12520-016-0362-8
Archaeological and anthropological data from Basel-Waisenhaus	Baumann et al. ²⁰	(N/A)
Groundwater data at Basel	Web Map Service Kanton Basel-Stadt	https://wms.geo.bs.ch/
Coring data	Basel administrative council	https://wms.geo.bs.ch/
Geological map	INSPIRE under Creative Commons Attribution 4.0 International (CC BY 4.0) license	https://download.bgr.de/bgr/Geologie/GK1000-INSPIRE/gml/GK1000-INSPIRE.zip
Digital Elevation Model	swisstopo	https://www.swisstopo.admin.ch/de/geodata/height/alti3d.html
Software and algorithms		
BWA v0.7.15	Li and Durbin ¹²⁸	http://bio-bwa.sourceforge.net/
DeDup v0.12.1	github.com	https://github.com/apeltzer/DeDup
DamageProfiler v1.1	Neukamm et al. ¹²⁹	https://damageprofiler.readthedocs.io/en/latest/index.html
Schmutzi v1.5.5.5	Renaud et al. ¹³⁰	https://github.com/grenaud/schmutzi
ANGSD v0.935	Korneliusson et al. ¹³¹	http://www.popgen.dk/angsd/index.php/ANGSD
bamUtil v1.0.15	Jun et al. ¹³²	https://github.com/statgen/bamUtil
SequenceTools v1.2.2	github.com	https://github.com/stschiff/sequenceTools
HaploGrep2 v2.4.0	Weissensteiner et al. ¹³³	https://haplogrep.i-med.ac.at/
yHaplo v1.1.2	Poznik et al. ¹³⁴	https://github.com/23andMe/yhaplo
Smartpca	Patterson et al. ¹³⁵	https://github.com/chrchang/eigensoft/
qp3Pop v650	Patterson et al. ¹³⁶	https://github.com/DReichLab/AdmixTools/
ADMIXTURE v1.3.0	Alexander et al. ¹³⁷	https://dalexander.github.io/admixture/
READ	Monroy Kuhn et al. ¹³⁸	https://bitbucket.org/tguenther/read
OxCal v.4.4.4	Ramsey ⁶⁰	https://c14.arch.ox.ac.uk/oxcal.html
QGIS v3.10.14	QGIS.org	https://www.qgis.org/en/site/
GRASS v7.8.5	1998-2022 GRASS Development Team	https://grass.osgeo.org

RESOURCE AVAILABILITY

Lead contact

Further information and requests for resources and reagents should be directed to and will be fulfilled by the lead contact, Margaux L. C. Depaermentier (m.depaermentier@unibas.ch).

Materials availability

All newly created datasets from this study can be found in [supplemental information](#). The Late Antique skeletal remains from Basel-Waisenhaus are stored at the Archaeological unit of the Canton Basel-Stadt (ABBS: Archäologische Bodenforschung Basel-Stadt, excavation number: 2010/11).

Data and code availability

- All raw data are available directly from [Table S1](#) of this paper. Genetic kinship data are directly available from the [Table S2](#) of this paper. aDNA raw data have also been deposited at the European Nucleotide Archive (ENA: PRJEB60689) and are publicly available as of the date of publication. Accession numbers are listed in the [key resources table](#). Reference datasets are listed in the [key resources table](#). The reference dataset for aDNA analyses derived from the David Reich Lab is cited in the [key resources table](#). Baseline strontium and oxygen data are available from Brönnimann et al. 2018 and Knipper et al. 2018.^{57,58} Baseline carbon and nitrogen isotope data are available from the Late Iron Age site at Basel-Gasfabrik⁸⁰ and from the Medieval (11th century AD) site at Basel-Barfüsserkirche.⁸¹ Anthropological and archaeological data are provided by Baumann et al. 2018.²⁰ References to the groundwater data, coring data, geological map and digital elevation model at Basel are provided in the [key resources table](#).
- This paper does not report original code.
- Any additional information required to reanalyze the data reported in this paper is available from the [lead contact](#) upon request.

EXPERIMENTAL MODEL AND SUBJECT DETAILS

Archaeological human samples

In this study, the eleven Late Antique skeletons discovered at the Basel-Waisenhaus burial ground were sampled for genetic, radiocarbon, and stable isotope analyses. Samples for radiocarbon dating, aDNA-analyses and C and N isotope analyses were taken from the eleven individuals, whereas only six individuals still possessed teeth that could be sampled for Sr and O isotope analyses. According to the morphometrical analyses of the skeletons, the burial group consisted of five infants (among them four possible males), one mature female, one possible mature female, two adult males, one possible mature male, and a further mature individual, whose biological sex could not be determined due to too many traumata on the pelvis.²⁰ The aDNA analysis enabled to precise this picture, providing a determination of the biological sex for most individuals. In total, the sample comprises therefore most probably two adult males, three mature females, one female infants and four male infants. Individual anthropological and genetic determination of the sex and age are reported in [Table S1](#). The sample size was too small, especially with respect to the age categories, to enable any sex-based analyses. No archaeological or biological information were available from this Late Antique context regarding each individual's gender. Hence, no gender-based analyses was conducted either.

Ethical statement

The Late Antique skeletons used for this study were discovered in the framework of rescue excavations carried out by the Archaeological unit of the Canton Basel-Stadt (ABBS, excavation number: 2010/11). Access to the skeletal material was provided by the ABBS and the sampling strategy was adapted to preserve the material as much as possible – for example by using samples from the same bones and teeth for various analyses. No living relatives are known for this community and no ethical issues exist related to excavation, conservation, analysis, and publication.

METHOD DETAILS

To interpret the results of the isotope and aDNA analyses in their cultural and environmental context, environmental analyses were conducted to understand the geographical and climatic settings at Basel for this period as well as to model potential land-use areas related to the graveyard. The anthropological and

archaeological analyses previously performed by M. Baumann and colleagues²⁰ were integrated into the interpretation of the data.

Environmental suitability analysis

A qualitative environmental analysis of the Waisenhaus graveyard catchment was carried out to predict the potential location of the corresponding Late Antique settlement, the associated croplands, and pastures.⁵⁹ The model was used to assess if the Sr isotope baseline suggested by Brönnimann and colleagues for the Iron Age site Basel-Gasfabrik, located 1.8 km away to the north-west (Figure 3), could equally be used for this study.⁵⁷ We used various environmental parameters to identify suitable settlement spots based on geological and pedological attributes, groundwater level anomalies, landscape accessibility, and permeability, as well as the potential premodern hydrologic system in a 1.5 km distance around the site. This activity sphere was thought to predict a self-sufficient crop cultivation strategy best. The strategy was based on the small population numbers per generation derived from the sample size of the graveyard and the chronological occupation of the site. However, the model does not depend on radial patterns around the site but on fuzzy analogies of the landscape represented in cost-distance relationships from a given location.^{57,72,139–141}

Groundwater at Basel was analysed using data from <https://wms.geo.bs.ch/> (last accessed 20th of November 2021), and a digital elevation model (DEM) was downloaded from swisstopo (<https://www.swisstopo.admin.ch/de/geodata/height/alti3d.html>, last accessed 20th of November 2021). Geological information was derived from 56 coring profiles (available from <https://wms.geo.bs.ch/>), which were evaluated and classified for surface conditions. The data was analyzed for geological/sedimentological composition (gravel, sand, silt, and clay deposits), groundwater level and bedrock, surface conditions, and potential soil development. Due to the extensive surface transformation of the city of Basel, no soil qualitative information is available for the urban area itself.

To predict the areas that accumulate the highest potential for settlement locations, groundwater depth, the interpolated geological suitability, and the distance from the graveyard were integrated into a qualitative model. The variables were merged using a focal approach with high values equaling high suitability and low values representing low suitability.⁵⁹ An accumulated friction surface was calculated to integrate the river channels, measuring the permeability of a given area based on topographic roughness. Eventually, a potential movement expenditure derived from the centre of the site at Basel Waisenhaus. This enables one to estimate landscape accessibility within a given radius around the site based on environmental permeability.

Radiocarbon dating

Samples for radiocarbon dating were taken from the eleven individuals, of which eight are left and three are right femora (Table S1). Radiocarbon dating (¹⁴C) of bone is predominantly obtained by dating collagen, i.e. organic C of the bone. Preservation of collagen, dependent on the burial location, is the major limiting factor in ¹⁴C dating of bones and has influenced the development of the methods to remove contamination.^{142,143} As shown by Brock et al. (2010), bones with N % lower than 1 have very poor collagen preservation.¹⁴³ At the ETH laboratory (Zürich, Switzerland), an ultrafiltration (UF) method, described by I. Hajdas and colleagues,¹⁴⁴ is applied. A recent study by Pawełczyk and colleagues (2022) has shown that slight modifications in the UF method result in consistent ages.¹⁴⁵ In short, the bones were washed and dried. At this point, a piece of an original bone was weighed (5–8 mg) for elemental analysis. If the N % > 1, ca. 400–800 mg of the bone was decalcified in acid, the organic insoluble was then treated with base to remove humic acid and gelatinized in acid solution at a higher temperature (60°C). The solution was then subjected to ultrafiltration to separate molecules of collagen > 40 kDa from humic contaminants, which have smaller molecules. The collected fraction was freeze-dried, and a portion of ca. 3.5 mg of dry gelatin was weighed for combustion in EA and subsequent graphitization in AGE system.¹⁴⁶ The graphite was pressed for the accelerator mass spectrometry (AMS) analysis using the MICADAS system at the ETH facility.¹⁴⁷

aDNA analyses

From the 11 graves, 14 samples were obtained from teeth or bones. At least one sample per skeleton (primarily the pars petrosal) was collected for aDNA analysis *in situ* during the excavation. The roots of the teeth sampled for Sr and O isotope analyses were sampled for further aDNA analyses where it was required. The surface was decontaminated by applying bleach for 5 minutes. After decontamination, the

powder was obtained by drilling. The extraction was performed with the method described by Krause-Kyora et al.¹⁴⁸ Established methods were used for sampling, DNA extraction and sequencing. In this study, only so-called shot-gun data were generated, which means that all the DNA that could be extracted was also sequenced. The samples sent for DNA analyses were handled in the laboratory following guidelines of aDNA work.¹⁴⁹ The DNA was extracted from the human remains, and partial uracil-DNA-glycosylase-treated sequencing libraries were prepared from all 14 samples.^{150,151}

Each library carries a combination of two indices as a unique identifier. All steps, including sampling, DNA extraction, and the preparation of sequencing libraries, were performed in clean-room facilities of the Ancient DNA Laboratory in Kiel. Negative controls were taken along for the DNA extraction and library generation steps. The resulting 14 libraries were submitted to shotgun sequencing on the Illumina HiSeq 6000 (2x100) platform. The generated sequencing data were mapped to the human genome build hg19 with BWA v0.7.15,^{152,128} using a lower mapping stringency (-n 0.01). Duplicated reads were removed with DeDup v0.12.1.¹⁵³

To assess the authenticity of the material, terminal deamination of reads was estimated with DamageProfiler v1.1^{154,129} (see [Figure S1](#) and [Table S1](#)). There was no sign of contamination in any of the samples, and the typical damage pattern used as an authentication criterion for aDNA was present (see columns “dmg 5p 1st pos” and “dmg 3p 3rd pos” in [Table S1](#) and [Figure S1](#)).

Additionally, Mitochondrial DNA and X chromosome contamination were calculated with Schmutzi v1.5.5.5¹³⁰ and ANGSD v0.935,¹³¹ respectively. All samples showed a deamination rate > 5 % at the first terminal positions and < 5 % contamination, patterns compatible with aDNA. The mapped data was trimmed with bamUtil v1.0.15¹³² (first and last two bases removed from every read) and pseudo-haploid genotypes on positions from the 1240 k panel^{155–157} were generated with SequenceTools v1.2.2 (<https://github.com/stschiff/sequenceTools>). Samples with < 20,000 covered SNPs were excluded from the population genetic analyses (n=3). Genetic sex assignment was performed by calculating the ratio of reads mapped to the sex chromosomes.¹⁵⁸ Mitochondrial and Y chromosome haplogroups were established with HaploGrep2 v2.4.0¹³³ and yHaplo v1.1.2,¹³⁴ respectively.

The generated pseudo-haploid genotype data were merged to a reference dataset (Allen Ancient DNA Resource (AADR): <https://reich.hms.harvard.edu/allen-ancient-dna-resource-aadr-downloadable-genotypes-present-day-and-ancient-dna-data>). A PCA was performed with smartpca,¹³⁵ using data of reference modern West Eurasian populations for the calculation of PCs (see [Figures 6](#) and [S2](#)). The remaining populations from the merged dataset were projected on the calculated PCs. Outgroup f3 statistics were performed with qp3Pop v650,¹³⁶ using Mbuti as an outgroup (see [Figure S3](#)). Unsupervised admixture analysis using three to six components was performed with ADMIXTURE v1.3.0¹³⁷ (see [Data S1](#)). Kinship analysis was performed with READ¹³⁸ (see [Table S2](#)).

Strontium and oxygen isotope analyses

Due to considerable post-depositional destructions, only six individuals still possessed teeth that could be sampled for Sr and O isotope analyses. For the infants, the deciduous tooth 84 was sampled. For the adults, two teeth (a first molar or a canine and a third molar) were selected in order to gain insights into the different life stages of the individuals. When possible, a second sample was taken from the roots of the teeth, which served as reference material. Sampling and sample preparation for Sr and O isotope analyses took place at the laboratory facilities at Integrative Prehistory and Archaeological Science (IPAS), Department of Environmental Sciences, University of Basel, and followed established protocols.^{159,160} For Sr and O isotope analyses, ca. 20 mg of enamel, taken from the upper third to the upper half of the growth axis, and ca. 10 mg of dentine, from each sampled tooth, were mechanically cleaned using a dental burr. Samples were cleaned in ultrapure water in an ultrasonic bath and ground to powder. For Sr isotope analysis, samples were dissolved in 1 ml 7 N HNO₃, dried down and re-dissolved in 2 ml 3 N HNO₃. Aliquots representing 3 mg of enamel (or dentine) were subject to ion exchange chromatography. After Sr separation using 70 µl of Eichrom Sr spec resin (50–100 µm) columns, the eluate was dried down and sent to the National Oceanography Centre, University of Southampton, for mass spectrometry. ⁸⁷Sr/⁸⁶Sr was analysed using a ThermoFisher Scientific Triton Plus Thermal Ionization Mass Spectrometer (TIMS). Two blanks that had been through the chemical procedure were < 0.1 ng. The long-term average for NIST SRM 987 on the instrument was 0.710245 ± 0.000027 (2 SD) on 214.

For O isotope analysis, ca. 1.5 mg of the powdered tooth carbonate samples and several replicated of 0.1 mg and 0.2 mg of carbonate isotope standards NBS 18, NBS 19 and USGS44 were weighed into 12 ml exetainers (Labco Limited, Lampeter, UK) without any pre-treatment and transferred to the mass spectrometry facilities at Aquatic and Isotope Biogeochemistry, Department of Environmental Sciences, University of Basel. The exetainers® with the carbonate samples and isotope standards were then purged with Helium (grade 5.0) for 1 hour, then acidified with phosphoric acid (100%), allowed to react for at least 90 minutes at 70°C, and analysed with a Gasbench II coupled to a Delta V Advantage mass spectrometer (Thermo Fisher Scientific, Bremen, Germany). For each sample and isotope standard six replicate injections out of the headspace in their respective exetainers®, using a 100 µl sample loop, were performed.

C and O isotopic ratios were calibrated using international carbonate isotope standards NBS 19, USGS44, and NBS 19 and NBS 18, respectively, and reported in δ-notation as δ¹³C and δ¹⁸O relative to VPDB (Vienna Pee Dee Belemnite). The analytical reproducibility of δ¹³C and δ¹⁸O, respectively (of the three isotopic standards, calculated as the standard deviation of δ¹⁸O of all replicate injections (n=36 per standard) in the analytical sequence, is ≤ ± 0.10 ‰. The analytical reproducibility of δ¹³C and δ¹⁸O of each sample, calculated as the standard deviation of δ¹³C and δ¹⁸O of six replicate injections per sample, is ≤ ± 0.10 ‰ in all but four samples, which show reproducibility between 0.11 ‰ and 0.12 ‰ for δ¹³C and between 0.11 ‰ and 0.14 ‰ for δ¹⁸O.

D. Brönnimann, C. Knipper, and colleagues have already determined a detailed and reliable map of bioavailable Sr and O for this region in the framework of the Basel-Gasfabrik project^{57,58} (Figure 3). Therefore, no additional baseline samples were analyzed for this study. However, the deciduous teeth of three infants were sampled from the burial place Basel-Waisenhaus, and because they may have died too young to have the time to change their place of residence after birth, their dental enamel ⁸⁷Sr/⁸⁶Sr values might be representative of the local Sr isotope signal as well. These values were compared to the existing baseline range of Basel-Gasfabrik. Moreover, a comprehensive environmental analysis was performed for Basel-Waisenhaus to ensure that the environmental settings within both catchment areas were similar.

Carbon and nitrogen stable isotope analysis

To preserve skeletal material, additional samples were taken for C and N isotope analysis from the same femora as for radiocarbon dating. Bone sampling and collagen extraction took place at IPAS. Sample preparation followed R. Longin¹⁶¹ with some modifications as described by C. Knipper, S. Reinhold and colleagues.¹⁶² Compact bone portions were cut, and the surfaces were removed. Ca. 700 mg of sample were demineralized in 10 ml of 0.5 M HCl, rinsed to neutrality and reacted with 10 ml of 0.1 M NaOH for 24 h, rinsed to neutrality and gelatinized in 4 ml of acidified H₂O at 70°C. Insoluble particles were separated using EZEE filter separators. The collagen was frozen and lyophilized. Samples were then transferred to Aquatic and Isotope Biogeochemistry, Department of Environmental Sciences, University of Basel, for mass spectrometry on an INTEGRA2 EA-IRMS instrument (Sercon Ltd., Crewe, UK). Analysis was conducted in duplicates.

Raw N and C isotope data were blank-, linearity-, and drift-corrected and then normalized to the Air-N2 and VPDB scales by means of two-point calibrations based on the international standards IAEA-N-2 and IAEA-CH-6 and an in-house EDTA standard. The resulting N and C isotopic compositions are reported in δ-notation as δ¹⁵N and δ¹³C in per mil relative to Air-N2 and VPDB, respectively. The reproducibility (1 SD) of the in-house and international isotope standards (EDTA, IAEA-N-2, IAEA-CH-6) was ≤ 0.18 ‰ for δ¹⁵N and ≤ 0.10 ‰ for δ¹³C. The difference between duplicate measurements ranged between 0.08 ‰ and 0.98 ‰ for δ¹⁵N and between 0.02 ‰ and 0.40 ‰ for δ¹³C, probably mostly reflecting various degrees of sample-related (in)homogeneity between duplicates. The reproducibility (1 SD) of a bone collagen sample (BAC 111), analysed as a long-term quality control sample once or twice in all sequences of bone collagen samples since 2016 was 0.26 ‰ for δ¹⁵N and 0.12 ‰ for δ¹³C.

QUANTIFICATION AND STATISTICAL ANALYSIS

A kernel density estimation model was run in the OxCal software v4.4.4⁶⁰ to improve the readability of the radiocarbon dates (raw data are available in the Table S1). After the algorithm removed these noises, the single-modelled dates showed a most probable total range of 40 years spanning from AD 370 to AD

410 (95.4 %, Agreement Indices of the model: 96.4) as shown in [Figure 5](#), with an error bar representing the mean value ± 1 SE.

To measure allele frequency correlations between populations, f3 statistics as defined by Patterson et al. (2012)¹³⁶ were conducted.

Mean and standard deviation values were calculated from Excel for Sr, O, C, and N isotope data (see [Table 1](#)). Human C and N isotope mean values were compared to faunal C and N isotope mean values from Iron Age and medieval Basel (see the [Table S3](#)).